F&E CAT

UCSD-SP-70-2

N70-40998

LONG TERM VARIATIONS IN HIGH-ENERGY GEOMAGNETICALLY TRAPPED PARTICLES

Sherman E. DeForest

Department of Physics
University of California, San Diego
La Jolla, California, 92037

A dissertation submitted in partial satisfaction of the requirements for the degree of Doctor of Philosophy in Physics
July 1970

DEC 1970
RECEIVED
NASA STI FACILITY
INPUT BRANCH

UNIVERSITY OF CALIFORNIA
SAN DIEGO

La Jolla, California

CASE FILE COPY

Department of Physics

Space Physics Group

NASA CONTRACT
Page III

UNIVERSITY OF CALIFORNIA

San Diego

Long Term Variations in High-Energy Geomagnetically Trapped Particles

A dissertation submitted in partial satisfaction of the requirements for the degree of Doctor of Philosophy in Physics

by

Sherman Edward DeForest

Committee in charge:

Professor Carl E. McIlwain, Chairman
Professor Gustaf Arrhenius
Professor W. Ian Axford
Professor Freeman Gilbert
Professor Barry Block

1970

The dissertation of Sherman Edward DeForest is approved, and it is acceptable in quality and form for publication on microfilm:

Committee Chairman

University of California, San Diego

1970

Dedicated

to the inhabitants of

Peña Springs

TABLE OF CONTENTS

		PAGE
LIST OF FIGURES		v
ACKNOWLEDGEMENTS		vi
VITA, PUBLICATIONS, AND FIELDS OF STUDY		vii
ABSTRACT		ix
I.	INTRODUCTION	1
	A. Characteristics of the Environment	1
	B. Origins of the Particles	5
	1. Neutron Decay	5
	2. Diffusion	6
	3. Other Sources	8
	C. Objectives of this Study	8
II.	DETECTOR	10
III.	DATA HANDLING	16
	A. Reduction	16
	B. ANAL	16
	C. Merging of Injun III and Explorer 15 Data	20
IV.	THEORY	24
	A. Diffusion Equation	24
	B. Transformation of the Solution of the Diffusion Equation	25
	C. Conversion of J to $\langle Q \rangle$	25
	D. Coordinates	27
	E. Boundary Conditions	27
	F. Determination of Γ	30
	G. Determination of Quality of Fit	32
V.	RESULTS AND CONCLUSIONS	37
	A. Equator	37
	B. $\Gamma(\lambda)$ and Electric Field Strength	41
VI.	SUMMARY	47
APPENDIX		48
REFERENCES		53

LIST OF FIGURES

FIGURE		PAGE
1	Time Variations of Trapped Protons	3
2	Omnidirectional Flux on January 1, 1965	4
3	Schematic Presentation of Detector "A"	11
4	Effective Geometric Factor of Detector "A" Versus Energy	12
5	Geometric Factor of Detector "A" Versus Spectral Index	13
6	Fits to Explorer 26 Counting Rates and the Derived Directional Fluxes	18
7	Contours in B-L Space of the Omnidirectional Fluxes Measured by the Combined Injun III and Explorer 15 Data	21
8	Contours in B-L Space of the Directional Fluxes Derived from the Injun III and Explorer 15 Data	23
9	Traces of Constant K in R-λ Space	28
10	Directional Flux for January 1, 1963 (R-λ)	33
11	Directional Flux for January 1, 1966 (R-λ)	34
12	Solutions on the Equator for Differing Forms of the Diffusion Coefficient	38
13	Ratio of Predicted to Measured Fluxes on January 1, 1966	42
14	Latitudinal Dependence of the Diffusion Coefficient	43
15	Omnidirectional Flux for January 1, 1963 (R-λ)	49
16	Omnidirectional Flux for January 1, 1966 (R-λ)	50
17	Directional Flux for January 1, 1966 (B-L)	51
18	Omnidirectional Flux for January 1, 1966 (B-L)	52

ACKNOWLEDGEMENTS

Throughout the course of this work, I have been constantly aware of the tremendous debt I owe to the many people responsible for the design, building, and successful operation of the spacecraft which I have used so freely. The previous existence of many of the data reduction programs was also a great help. Not only was Dr. C. E. McIlwain instrumental in all of the above, but he has also aided and encouraged me personally in my studies.

Also of great importance has been the continuing exchange of ideas between myself and the ever-optimistic Carl Rindfleisch who has cheered many a gloomy day. Conversations with Anil Davé and Stephen Rearwin have been a great help.

Several people have aided in assembling the final version of this work. In particular, Mrs. Wanda Hildyard efficiently and expeditiously typed the manuscript, and Mrs. Patricia Gifford prepared many of the figures. I am grateful to both.

I would like to thank Dr. Daniel Schwartz for pointing out the beneficial qualities of E′, but it is just not my style.

The computations in this work were done at the UCSD Computer Center. Many thanks are due the UCSD Chapter of the SDS for not burning this facility before I had finished my many labors there.

Lastly, and in deep felt earnestness, I acknowledge the generous support of the American people through the offices of the Department of Agriculture and NASA Grant NGL 05-005-007 and Contract NAS 5-10364.

VITA

February 11, 1939 - Born - Toledo, Ohio, U.S.A.

1961 - B.S., Michigan Technological University, Houghton, Michigan

1962 - M.S., Michigan Technological University, Houghton, Michigan

1962 - 1964 - Space Sciences Laboratory, Litton Industries, Inc., Beverly Hills, California

1964 - 1970 - Research Assistant, Department of Physics, University of California, San Diego La Jolla, California

PUBLICATIONS

"Flexagons," Michigan Tech Engineer, 2, 22 (1960).

"Energy Transfer in Jack Pine as Related to Infrared Reflectivity of Cones, Bark, and Needles," Master of Science thesis, Michigan Technological University, Houghton, Michigan (1962).

"Effects of Different Field Expansions on Omnidirectional Proton Counting Rate Data," JGR, 71, 3273 (1966).

"Use of Electronic Computers to Aid in the Design of Satellite-Borne Experiments," S. E. DeForest, and R. J. Walker, Department of Physics, University of California, UCSD-SP-67-3 (1967).

"The UCSD Plasma Detector on ATS-5," C. E. McIlwain, and S. E. DeForest EOS, 50, 660 (1969).

"Initial Results of ATS-5 Plasma Experiment," EOS, 50, 660 (1969).

"Precipices and Chasms in the Magnetospheric Plasma," EOS, 51, 390 (1970).

"Plasma Clouds in the Magnetosphere," C. E. McIlwain and S. E. DeForest, Department of Physics, University of California, UCSD-SP-70-1 (Presented at International Symposium on Solar-Terrestrial Physics held at Leningrad, USSR, May 1970).

FIELDS OF STUDY

Major Field: Physics

Studies in Applied Mathematics.
Professor Jacob Korevaar

Studies in Classical Electrodynamics
Professors Leonard N. Liebermann and Walter Kohn

Studies in Advanced Mechanics
Professor Nguyen-Huu Xuong

Studies in Quantum Mechanics
Professor David Y. Wong

Studies in Nuclear Physics
Professors Maria Goeppert Mayer, Keith A. Brueckner, and William R. Frazer

Studies in Statistical Physics
Professors Harry Suhl and Morris Weger

Studies in Advanced Electronics
Professor Laurence E. Peterson

ABSTRACT OF THE DISSERTATION

Long Term Variations in High Energy
Geomagnetically Trapped Particles

By

Sherman Edward DeForest

Doctor of Philosophy in Physics

University of California, San Diego, 1970

Professor Carl E. McIlwain, Chairman

The omnidirectional flux of geomagnetically trapped protons of 40-110 Mev has been measured by identical detectors on board three spacecraft (Injun III, Explorer 15, and Explorer 26) from 1963 to 1966. This data is shown to be consistent with a model of protons diffusing by violation of the third adiabatic invariant. The derived diffusion coefficient is $D(L,\beta_o) = 1.32 \times 10^{-7} L^6 e^{.27} (5.6+\sin\beta_o)(1.0-\sin\beta_o)$ (Re^2/day) where β_o is the equatorial pitch angle, and L is the McIlwain shell parameter. This form of $D(L,\beta_o)$ is consistent with diffusion driven by a randomly varying electric field of approximately 0.5 mv/m and auto-correlation time of the order of tens of seconds.

I. INTRODUCTION

The Problem: In this study, we address ourselves to the problem of the existence of large numbers of energetic protons trapped deep in the earth's magnetosphere. Specifically, we explore the possibility of radial diffusion inward from outer space, and determine the possible nature of such diffusion.

Throughout the following discussion, high-energy geomagnetically trapped protons will be defined as particles of 40 to 110 Mev energy. Spatial location of the particles will be specified by a non-local time dependent B-L` coordinate system or the derived R-λ system (McIlwain, 1966a). Flux will be defined as being the omnidirectional flux, differential in energy, which has been integrated over the energy range 40 to 110 Mev. Particle flux which is differential in energy will always be labeled as differential flux. Perpendicular or directional flux will be defined as the flux normal to the local magnetic field line.

A. Characteristics of the Environment

High-energy protons trapped in the earth's geomagnetic field were unambiguously identified and studied very early in the history of space exploration (Freden and White, 1959). During the early sixties, several experimenters measured the flux of these particles, and several theories were put forward to explain the existence of the surprisingly large numbers of them (Hess, 1968, Chapter 4). However, these particles exhibit other interesting properties in addition to

their numbers. Unlike the electron population and the lower energy particles of both signs which fluctuate in density over orders of magnitude (Hess, 1968; Yeager and Frank, 1969; DeForest, 1970; McIlwain, 1970), they remain remarkedly stable in time as is demonstrated in Figure 1, which is a plot of the flux as measured on the spacecraft Explorer 26. Note that the flux slowly decreases, but does not show any rapid changes. Because of this very slow evolution, a single spacecraft can map out a large area in B-L space and be sure of getting a representative picture. One such mapping is shown in Figure 2 for R-λ space. The data has been normalized to January 1, 1965 by a method to be described in Section III. Figure 2 represents a "snapshot" of the proton flux at a given time even though the data was actually gathered over a period of weeks. As in Figure 1, this data was taken from Explorer 26, one of three spacecraft used in this study.

Experimenters working with Explorer 7 showed at least for the relatively low values of L less than 1.6 that the high energy protons did not respond to solar flares (Pizzella, et al., 1962). Unfortunately, this detector responded to electrons of energy greater than 1.1 Mev. Therefore, measurements further out in L are contaminated by the large electron population. At higher L values, rapid nonadiabatic changes in the flux of trapped protons have been seen in association with large geomagnetic storms (McIlwain, 1964). These changes consist uniformly of decreases in the flux which can reach an order of magnitude at L = 3, but they are not observed below L = 2.2. Solar protons

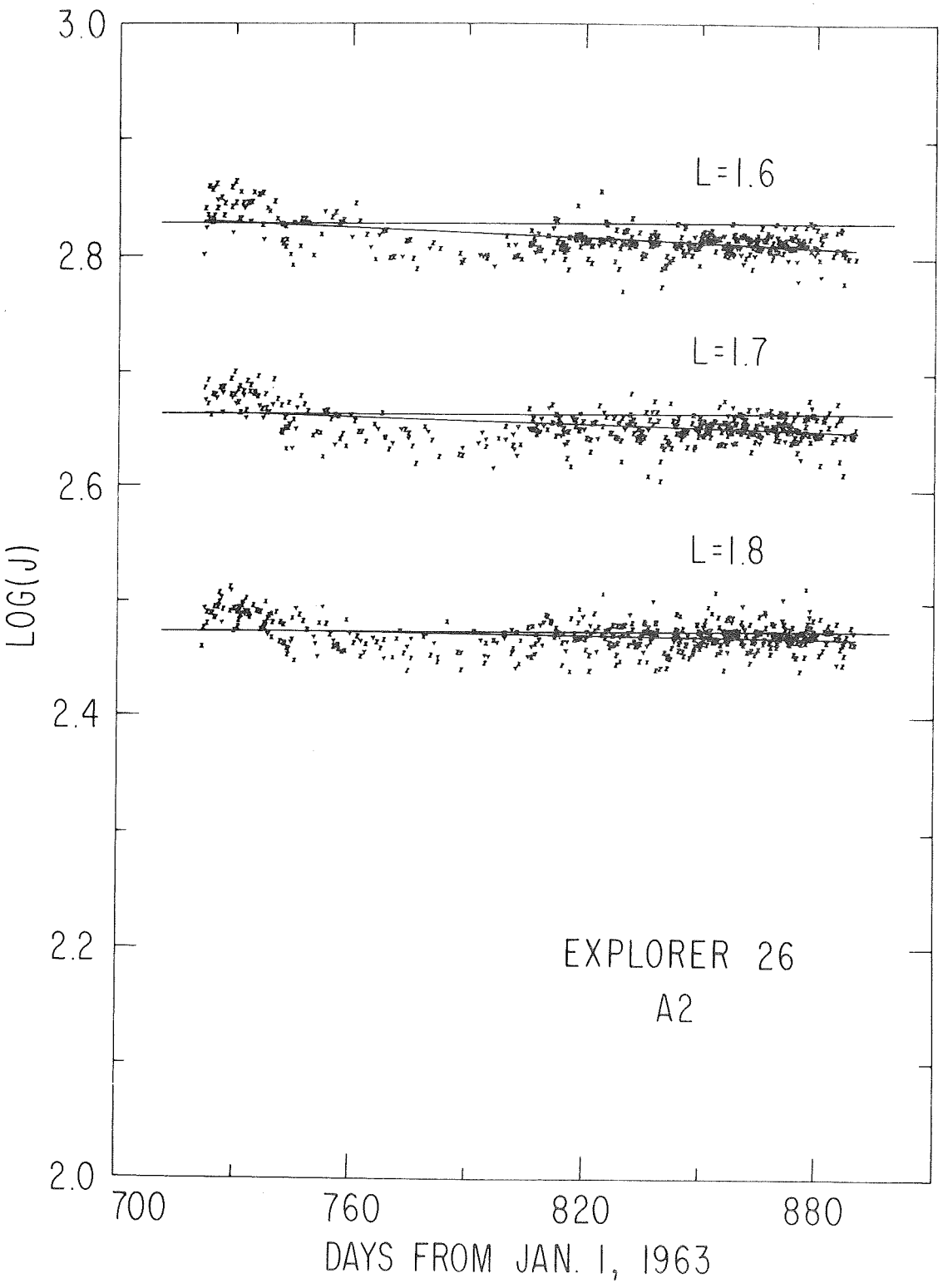


Figure 1 Time Variations of Trapped Protons

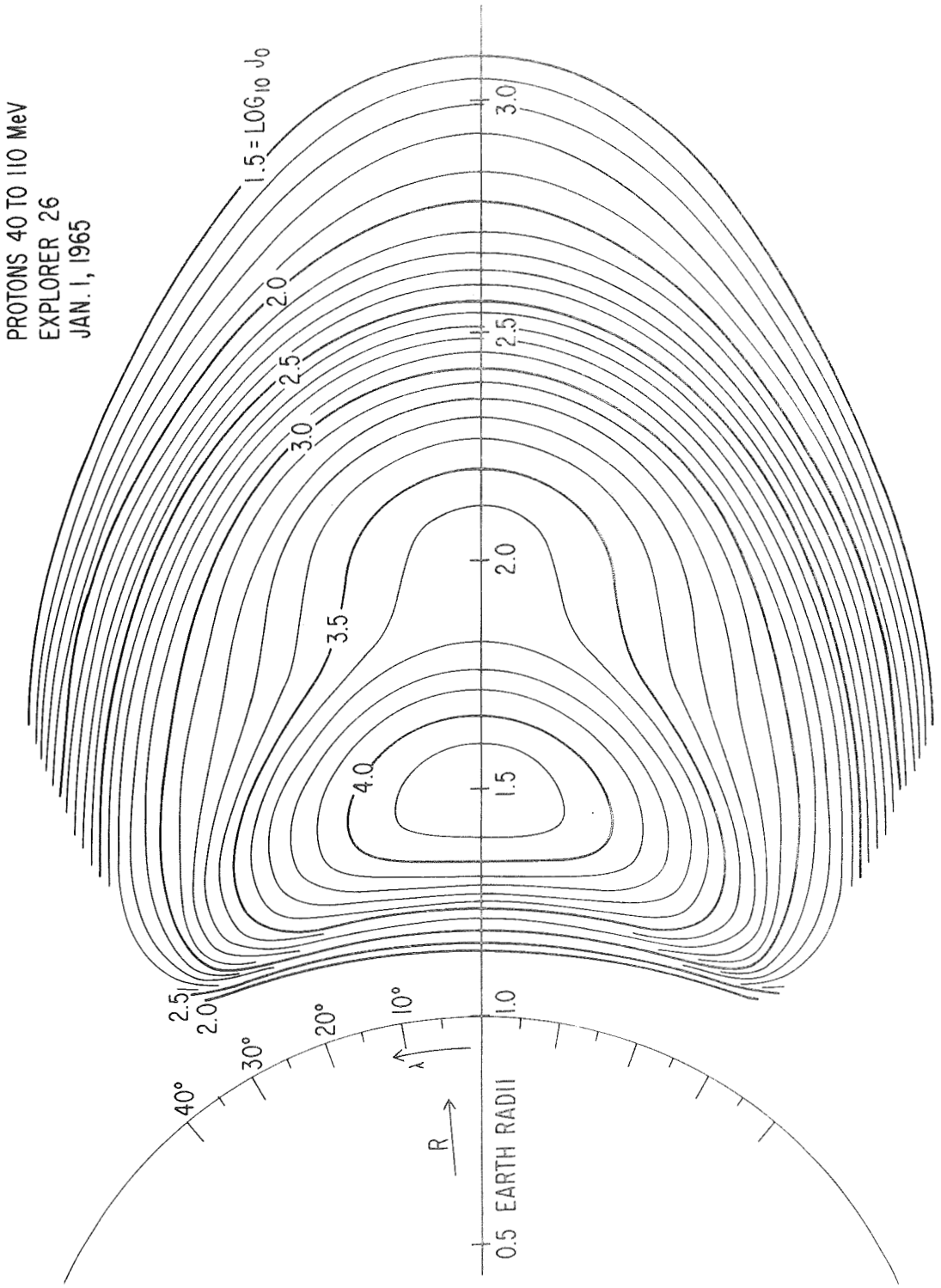


Figure 2 Omnidirectional Flux on January 1, 1965

have been seen to penetrate to L = 4 by Fillius (1968). However, he states that these particles show no signs of merging with the trapped radiation. All indications are that these particles which penetrate directly from the sun are not important members of the flux, particularly at L less than 3. Therefore, this class of protons will not be considered in the following discussion.

B. Origins of the Particles

1. Neutron Decay

Several authors have tried to explain the presence of trapped protons as being due to the decay of neutrons produced in the upper atmosphere--the cosmic-ray albedo decay theory or CRAND (Hess and Killeen, 1966; Dragt, et al., 1966). Some very suggestive experimental evidence supports this theory. For instance, it was used to predict the shape of the energy spectrum for at least one point in space quite successfully (Freden and White, 1960). Blanchard and Hess (1964) ambitiously tried to predict the proton population over a complete solar cycle using CRAND as a source. However, detailed calculations by all of these authors indicate that this source is much too weak to explain all the trapped protons. While one is forced to admit that the physical parameters involved are not well known, recent measurements on board OGO-F support the contention that CRAND is much too small to be the origin of the high energy protons (Jenkins, 1970).

Neutron decay will be discussed further in a brief comparison with diffusion in the Summary.

2. Diffusion

The most promising theory of the origin of trapped protons was apparently put forward by Kellogg (1959) and Parker (1960). They both proposed that protons diffused inward conserving the first two adiabatic invariants (Northrup and Teller, 1960). The third invariant could be broken by either magnetic fluctuations or varying electric fields. The theoretical development of diffusion as applied to high energy magnetospheric particles is presented in detail in Section IV. Throughout this paper, the term diffusion will be applied to the particular one dimensional type of diffusion produced by violation of the third adiabatic invariant. In this section we consider qualitatively other work that has been done on diffusion.

The first problem one faces in trying to study any type of diffusion in the magnetosphere is the fact that a single particle or group of particles cannot be followed through space. Instead, some idea of the nature of the diffusion coefficient has been gained by observing certain morphological features move after geomagnetic disturbances. Several objections have been raised to this procedure since it requires special cases to work. Nevertheless, results are obtained which tend to agree with both theoretical work and other experimental techniques (See Fälthammar, 1969, for a recent review of this approach).

Other indirect evidence of diffusion was provided by the detectors on board Explorers 12 and 14, which measured the spectral shape of protons from .1 to 5 Mev. These data could be fit with a curve of the form

$$J(>E) = k[\exp(-E/E_o)] \quad (1)$$

for a given location in space. When comparing spectra at different locations, the interesting result that

$$E_o \propto L^{-3} \quad (2)$$

was found for particles on the equator (Davis and Williamson, 1963). This result is predicted by a model of particles drifting in radius while maintaining a constant magnetic moment (first adiabatic invariant).

Another indication of diffusion was described by Nakada, et al. (1965). They argued that the particles could be shown to have had a common origin in space by using information about pitch angles and then applying Liouville's theorem to the distribution.

Newkirk and Walt (1968) chose instead to analyze the time variations of particles (electrons, in this case) by fitting the observed data to appropriate diffusion equations. As will be seen shortly, the present approach is similar.

Davis and Chang (1962) as well as Nakada and Mead (1965) tried to derive the magnitude and functional form of the diffusion coefficient, assuming that magnetic variations drove the diffusion. Both studies concluded that magnetic fluctuations seem to produce a diffusion rate which is too small by as much as an order of magnitude. A more likely source might be electric field fluctuations. Birmingham (1969) discusses diffusion produced by convection electric fields in the magnetosphere and points out that much larger diffusion coefficients can be derived from reasonable physical assumptions about the process. The

possibility exists of deciding unambiguously between the two hypothetical driving forces because the diffusion constant decreases rapidly for nonequatorial particles in the magnetic case, but not in the electric case (Fälthammar, 1968). This idea is developed further in Section IV.

3. Other Sources

Although the neutron decay and diffusion theories have been the most successful in predicting physical effects, other theories have been advanced. For instance, Akasofu (1964) suggested that neutral hydrogen from the sun could penetrate deep into the magnetosphere before becoming ionized by charge exchange. This idea and others are discussed by Hess (1968, Chapter 3). All have serious faults and will not be presented here.

C. Objectives of this Study

The objectives of this study can be stated quite simply:

(1) investigate whether or not the data is consistent with diffusion by violation of the third adiabatic invariant,

(2) determine the diffusion coefficient as a function of spatial position, and

(3) attempt a physical explanation of the diffusion based on the nature of the diffusion coefficient.

A large body of data is available at the Space Sciences Laboratory of the University of California at San Diego for the study of high energy protons. Data from Injun III, Explorer 15, and

Explorer 26 were selected for this work. These spacecraft carried identical detectors, and had useful lifetimes ranging from 1962 to 1966. This lifetime is especially important since, as we saw in Figure 1, long baselines must be recorded if we are to see large changes in the counting rates. The method of attack is to simulate as closely as possible the population of protons on January 1, 1963, establish reasonable boundary conditions, and calculate predicted counting rates on January 1, 1966, using a family of diffusion constants. The predicted rates are then compared to the measured rates to select the magnitude and functional form of the coefficient which best matches the data. Even with their long time span, the average counting rates in 1966 are nearly equal to those in 1963. The maximum ratio of initial to find rates is about a factor of three.

The detector and spacecraft are described in the next section. The method of data handling is described in Section III, and a detailed development of the theory is presented in Section IV. Results are given in Section V, and conclusions derived from them.

II. DETECTOR

A schematic representation of the detector used is shown in Figure 3. It consists of a spherical plastic scintillator 0.4 cm. in diameter connected by a conical light pipe to a photomultiplier. The front 2π steradians seen by the scintillator are shielded by a uniform 1.8 g/cm^2 of aluminum. The shielding over the back 2π steradians was estimated from the spacecraft construction. This detector is called the "A" detector. It has outputs from two discriminators called "A1" and "A2". Throughout this study, only data from A2 is used since A1 responded to electrons in addition to the desired protons. For further details of construction, the reader is referred to both the previously mentioned article by Fillius (1968) and one by McIlwain (1966b).

The response of the detector is seen in Figures 4 and 5, which were taken from the same paper by Fillius. Using Figure 4, one can show that for a power law spectrum of the form $J(E)dE = KE^{-N}\,dE$, A2 approximates a rectangular bandpass of 40 to 110 Mev. Figure 5 shows how the effective geometric factor varies with the spectral parameter, N. This curve becomes important for converting counting rates to flux for comparison over large regions of space where N may change considerably. The average geometric factor often cited for this detector is 1/18 cm^2, which is equivalent to N = 3. However, N varies from 1.5 to 4.5 in the region considered here. Therefore, the average value is not used. This matter is discussed further in Section IV.

The design of detector A is particularly well suited for intercomparison of counting rates between detectors on different spacecraft.

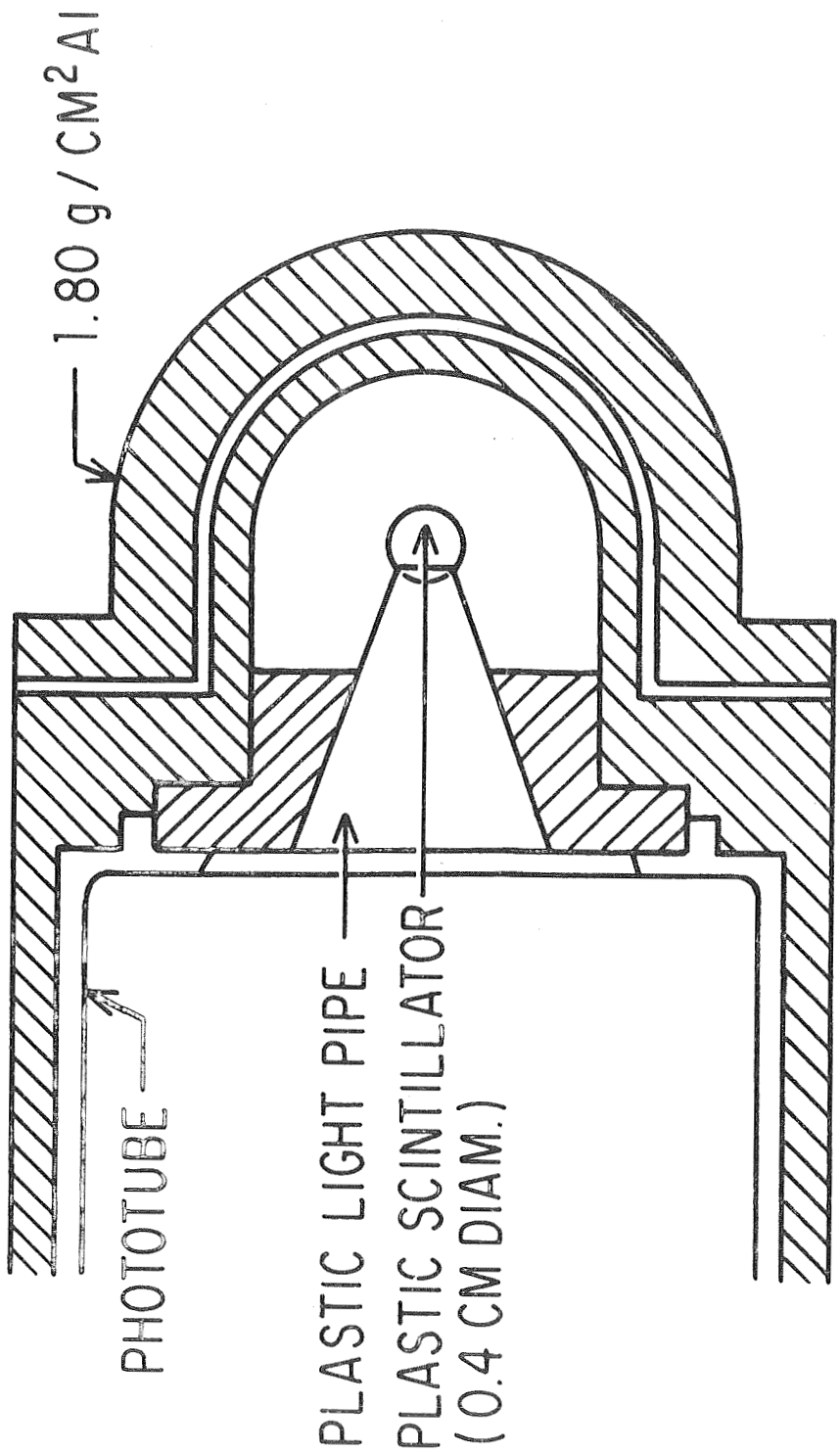


Figure 3 Schematic Presentation of Detector "A"

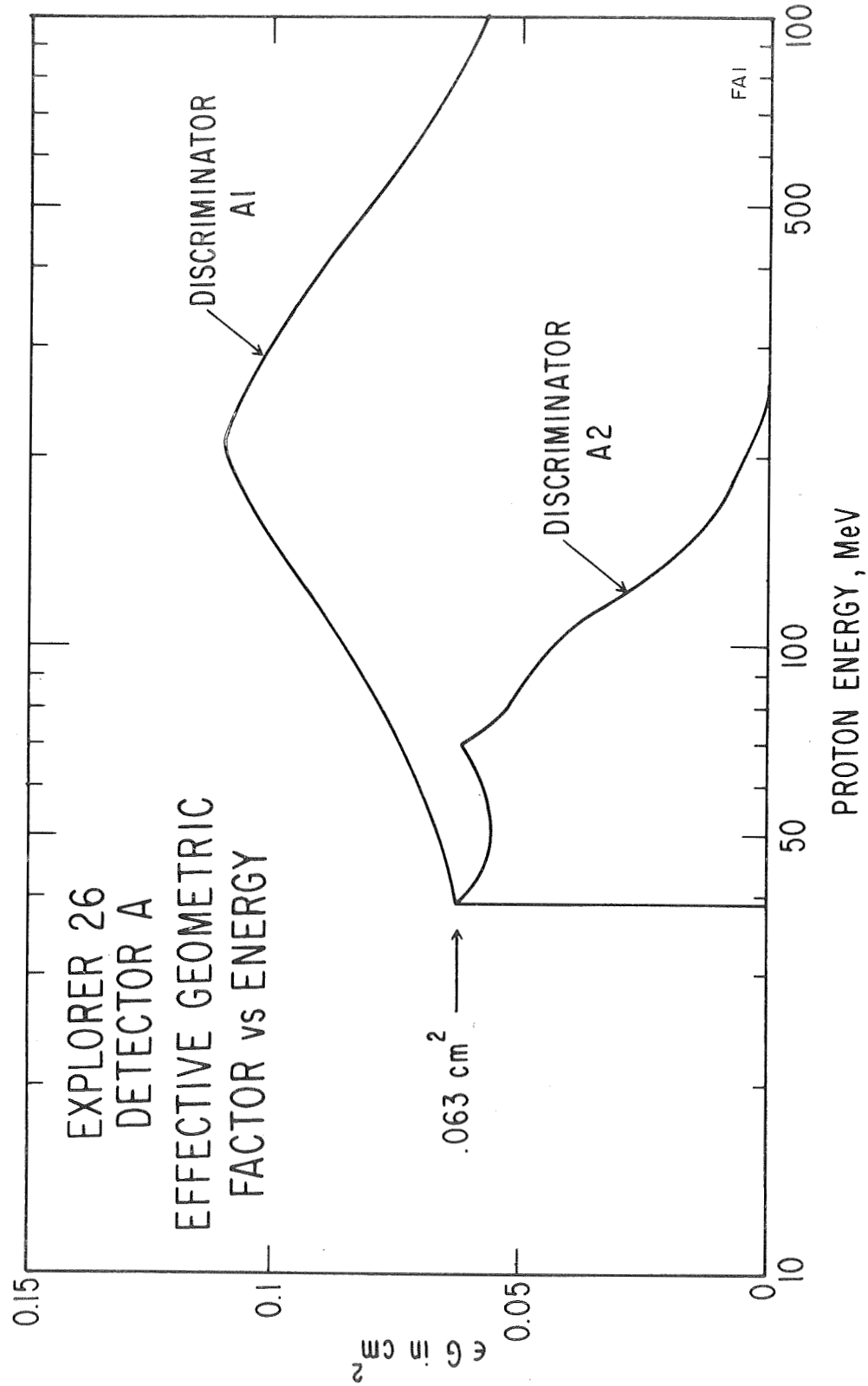


Figure 4 Effective Geometric Factor of Detector "A" versus energy

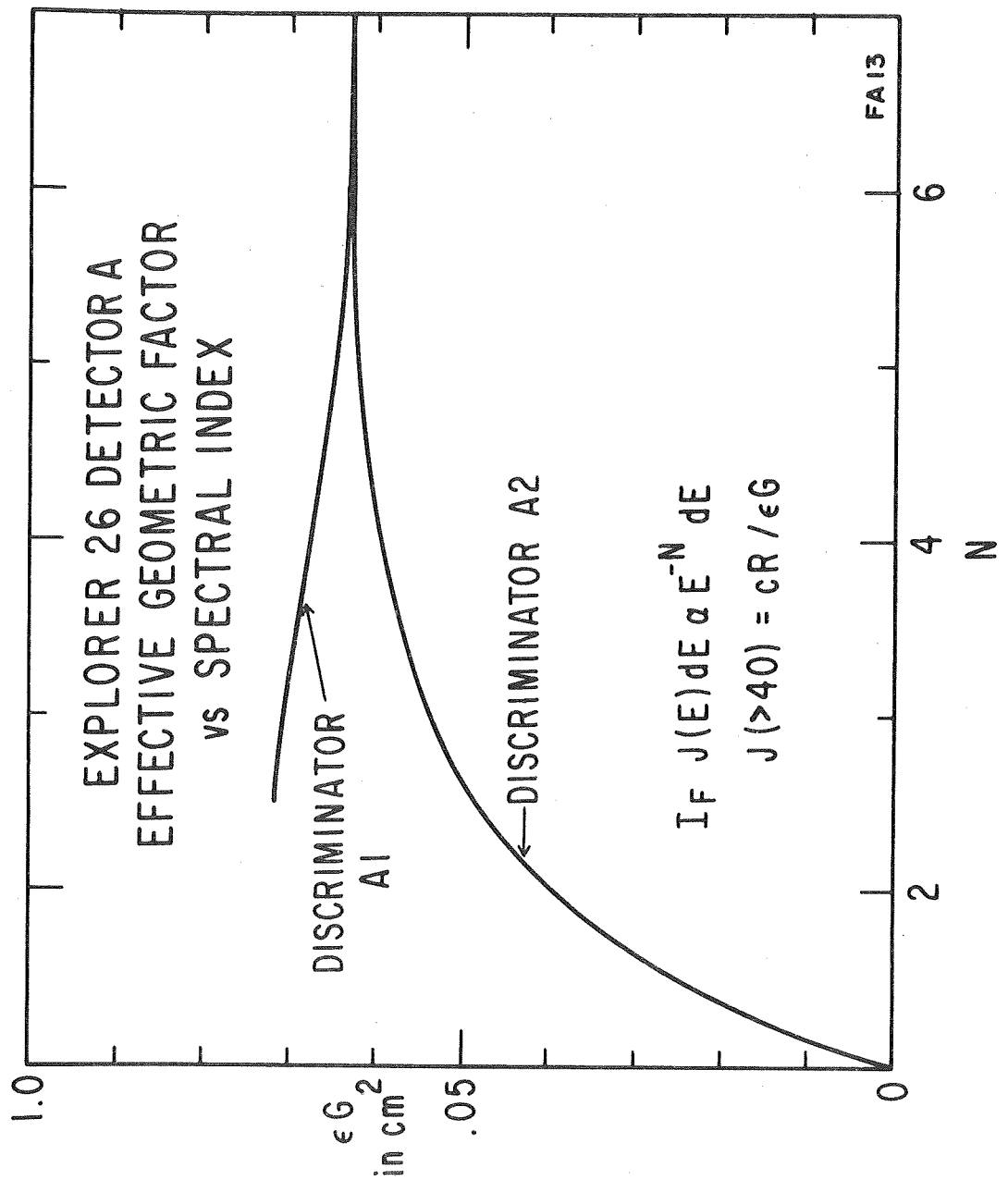


Figure 5 Geometric Factor of Detector "A" Versus Spectral Index

The threshold energy is set primarily by the thickness of the shielding, and not the level of discrimination. The shielding is easily made and remains stable in use. If the threshold had depended on the electronics, there might be serious questions about the reliability of the calibration after a few months in space. The upper limit of discrimination is not nearly so serious since the spectrum is a rapidly decreasing function of energy. In fact, the counting rates from A1 are only about 25% higher than those from A2 in those regions of space where there is no electron contamination. From this we see that small changes in the upper limit of discrimination, if they exist, will not seriously affect the counting rates.

Minimum resolving time for the detector is set by the telemetry constraints. In all three spacecraft considered, this time is of the order of a minute or less. Since the variations in counting rate are of a much longer period, the resolving time of the detector does not influence the data. The net deadtime associated with the detector and its electronics is approximately .25 μsec. The highest counting rates observed in this study are about 10^4 per second. Therefore the deadtime correction is .25 per cent at a few places and very much smaller on the average. Since this is smaller than other sources of error such as the B-L coordinate system itself (DeForest, 1966), deadtime corrections will also be ignored.

Data from Injun III was normalized to January 1, 1963 and combined with data from Explorer 15, which had been normalized to the same date. Since Injun III was a low altitude, high inclination spacecraft (Van Allen, 1966), and Explorer 15 gave data out to 4 earth

radii and ± 30° magnetic latitude (McIlwain, 1966b), the resulting combination yielded coverage over all B-L space out to L = 3.

Explorer 26 was launched in December, 1964 into an orbit of apogee 5, perigee .047 earth radii, and inclination 20°. No polar orbiting spacecraft was available with a similar detector, so coverage provided by this spacecraft is somewhat more limited in spatial extent than the January 1, 1963 data. Also an encoder failure limited the usefulness of this instrument. However, enough data was recovered to make proton mappings for both January 1, 1965 and 1966 by careful editing.

To do a diffusion study, a further piece of experimental information is needed--the spectral parameter mentioned above. The "A" detector does not return this information, but fortunately, Lavine and Vette (1969) published a complete mapping of N over the region of interest. Many spacecraft and experiments were involved in providing the basic information used. Therefore, it is assumed that the results represent the best estimate of the spectral parameter. By appropriately combining N with the counting rates from detector "A", one can calculate the differential flux at a given location in space. That is one boundary condition needed to solve the diffusion equation. The other boundary conditions will be discussed in Section IV.

III. DATA HANDLING

A. Reduction

Data from the various spacecraft are received by selected ground stations, recorded on analog magnetic tape, and sent to Goddard Space Flight Center in Greenbelt, Maryland. There, digital tapes are made and sent to the experimenters. At UCSD, these tapes are then sorted, combined and edited. The editing process removes both data points which have been affected by bad telemetry and duplicated data points due to simultaneous coverage by more than one ground station. Next, data is interpolated to certain standard values of L and stored in order of increasing B on other magnetic tapes. The format of these final tapes has been chosen to allow easy access to the data. Therefore, these tapes make an effective, compact working library.

Although the original data tapes are available, no purpose would be served by using them in this study. Therefore, all results presented here are based on the final reduction tapes.

B. ANAL

ANAL is a complex data handling program which was originally written to reduce Relay I data. Relatively minor changes have been necessary to use this program on other spacecraft. In brief, ANAL reads in specified data, performs any necessary corrections to the counting rates such as temperature and background corrections, and then fits the data to a standard expansion in both time and magnetic field for discrete values of L. The data and fitted curves can be both plotted and printed. Coefficients of the expansion are punched

out on cards along with selected relevant information (such as the time span considered in making the fit). A sample plot of this type is shown in Figure 6. Also, Figure 1 was made by the same program using an option for time plotting. Figure 2 was made by another program which used sets of cards punched by ANAL.

The fit selected for this study is of the form

$$\mathrm{Log}(J) = A_1 + A_2 t + \sum_{3}^{8} A_n b^{n-2} \qquad (3)$$

where J is the omnidirectional flux of particles, t is the time, and $b = B/B_o$ (The convention of B_o designating the minimum B along a given line of constant L will be observed. Such a fit is made for each of the standard values of L.

In order to simplify the specification of the time, a special calendar has been adopted for use within the Space Sciences Laboratory. This calendar starts with day 1, defined as January 1, 1963. Days are accumulated serially from that date. In normal use, time is specified as the day and fraction of day. The number so specified is referred to as the Monterey date, and the calendar is called the Monterey calendar (Playboy, 1963; and R. W. Fillius, private communication).

Knowledge of the omnidirectional flux along a line of force allows one to calculate the perpendicular flux along that line (Farley and Sanders, 1962; Roberts, 1965). Details of this transformation will not be discussed here. However, it should be noted that the accuracy of the transformation depends approximately on the accuracy with which the first derivative of J along the line of force is known. After

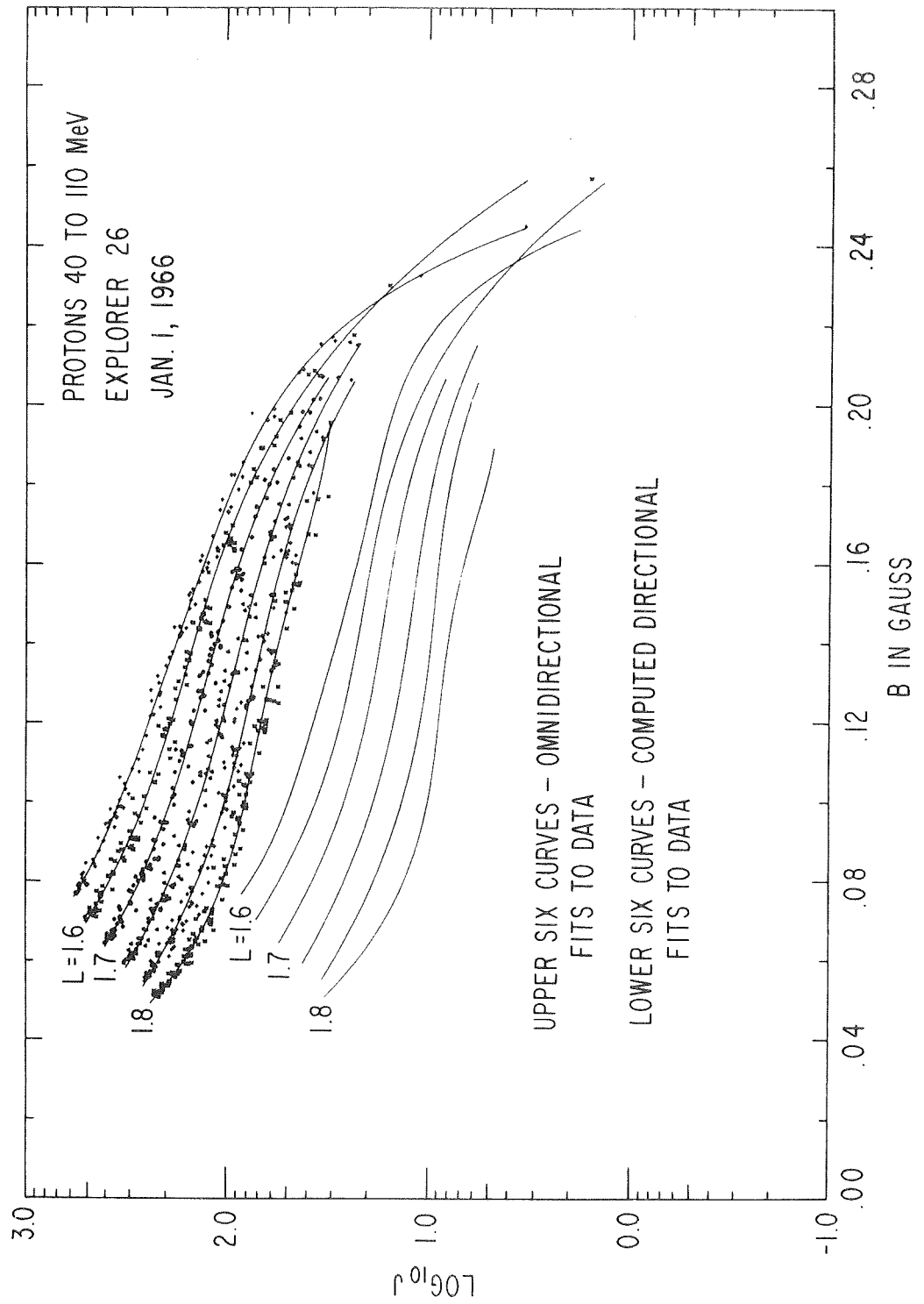


Figure 6 Fits to Explorer 26 Counting Rates and the Derived Directional Fluxes

fitting the data, ANAL makes this transformation and punches cards for the expansion of the directional flux in the same manner as for the omnidirectional flux. A typical example of such derived curves is shown in Figure 6 along with the omnidirectional flux.

ANAL has one potential shortcoming in the way it fits the data. The form shown in equation (3) does not allow for the easy handling of zero counts. Therefore, ANAL ignores all such readings. This creates an error at low counting rates. To assess the effect of this error, consider a system which counts random events with an average occurrence of λ per reading. Then the probability, $w(n)$, that n counts per reading will occur is given by Reif (1965, p. 41)

$$w(n) = \lambda^n e^{-\lambda}/n! \tag{4}$$

Let us now ask what the average counting rate would be if over some long period of time, T, we accumulate events over many small intervals, and divide the total accumulated events by the time $T-T_o$, where T_o is the sum of all accumulation periods with zero counts. Call this new rate λ'.

Then we can write

$$\lambda' = \lambda T/(T - T_o). \tag{5}$$

However, this last expression is seen to simplify to

$$\lambda' = \lambda/(1 - w(0)) \tag{6}$$

or

$$\lambda' = \lambda(1 - e^{-\lambda}). \tag{7}$$

Therefore, λ and λ' are equal for all practical purposes at high counting rates. In fact, even if λ gets as small as 5, they are still equal to within 1 per cent. Counting rates used in this study get that low only at the outermost steps in L. As was seen in Figure 6, the RMS deviation of the data points about the fitted curves are of the order of a few per cent. Since that is many times greater than the error that could be introduced by neglecting zero count readings, we may proceed with confidence in the fitting technique.

C. Merging of Injun III and Explorer 15 Data

This study started with the effort to produce a comprehensive mapping of the protons by combining data from Injun III and Explorer 15. As mentioned in the previous section, the spatial coverage of each spacecraft compliments the other. Because of the difficulties of writing a program to merge the data directly, much of the work was done by hand. Contour plots in B-L space were made for each spacecraft. Then the graphs were overlaid and a tracing made of the combination. Fortunately, the fluxes in the overlap region agreed quite well. The maximum difference was approximately 10 per cent, and that was in the cut-off region where the fluxes are changing rapidly with L. Figure 7 shows the results. The interpolated part of the combined graph was obtained by extending the appropriate contours until they met. No attempt was made to extend analytically the fits beyond the domain of the data fitted. However, the resulting contours had to be put into a more usable form for diffusion studies. Therefore, values of the combined contours were punched up on a set of cards

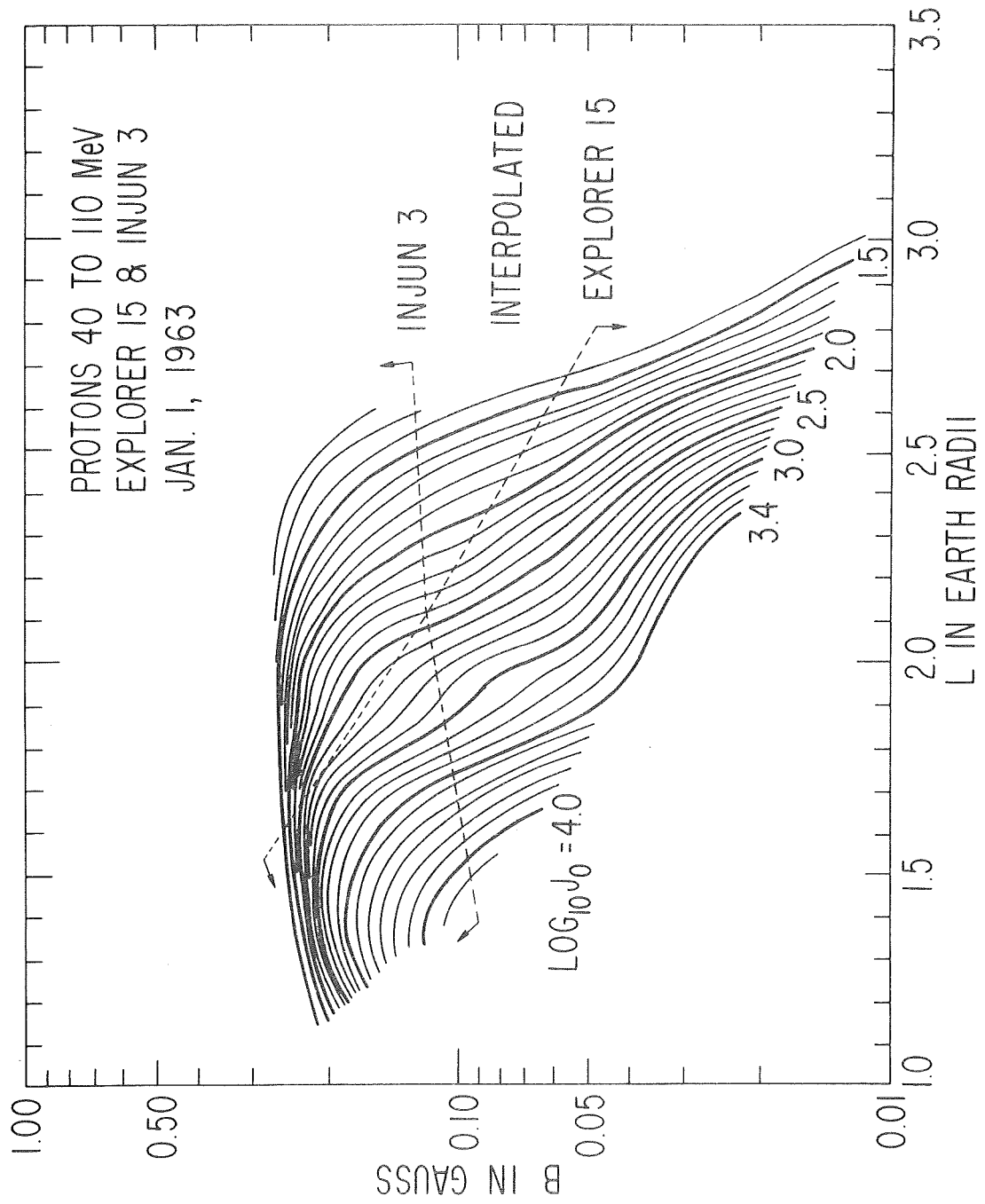


Figure 7 Contours in B-L space of the Omnidirectional Fluxes Measured by the Combined Injun III and Explorer 15 Data

which were used as the input to a specially modified version of ANAL. Both omnidirectional and directional contours were then generated in the normal way. The contours of directional flux are shown in Figure 8. The reconstructed omnidirectional contours are identical to those in Figure 7.

As a final note, it should be mentioned that a subroutine was written called POWER which contains the spectral information in the paper by Lavine and Vette (1969). When called by a location in B-L space, POWER returns the appropriate value of the spectral index, N.

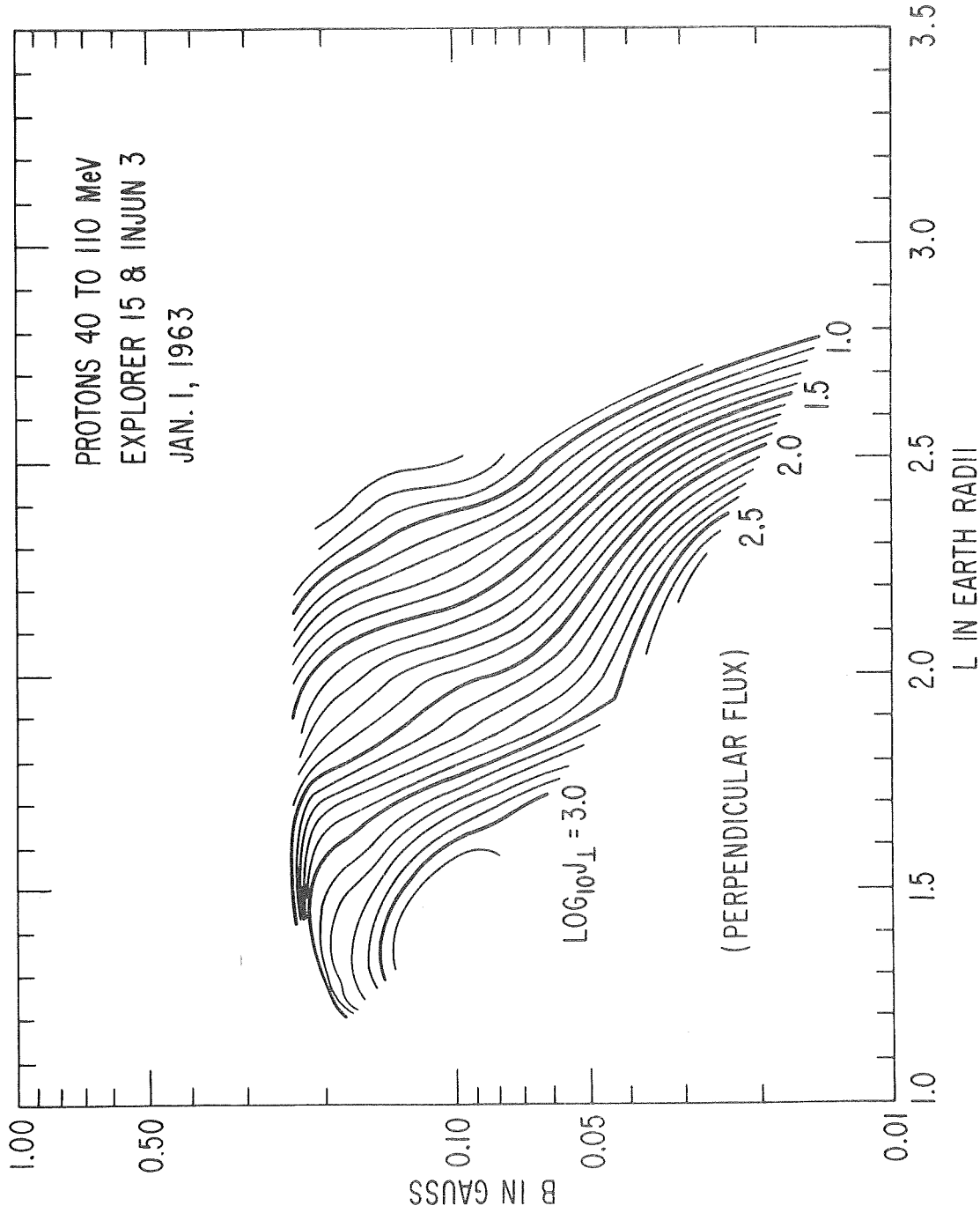


Figure 8 Contours in B-L Space of the Directional Fluxes Derived from the Combined Injun III and Explorer 15 Data

IV. THEORY

A. Diffusion Equation

Although the motion of high energy protons in the magnetosphere is properly described by means of the Fokker-Plank equation, Fälthammar (1966) found a relation between the two Fokker-Plank coefficients which enables one to cast the equation into "diffusion-like" form with only one coefficient. Even with this simplification, the diffusion equation can appear in several forms depending on the space in which one chooses to work. For this study, a form similar to the one used by Birmingham (1969) is the most convenient.

$$\frac{\partial \langle Q \rangle(\alpha, M, J, t)}{\partial t} = \frac{\partial}{\partial \alpha}\left[D_{\alpha} \frac{\partial \langle Q \rangle}{\partial \alpha}\right] + S \tag{8}$$

where M and J are the first and second adiabatic invariants respectively, t is the time, and $\langle Q \rangle$ is the longitudinal average of the guiding center density defined for the four dimensional space, (α, β, M, J). β is longitude. S is the distributed sink or source of particles. Its form in this coordinate system need not be discussed because one of the assumptions to be made is that $S = 0$. Finally, $\alpha = -\mu/L$ with μ being the magnetic dipole moment of the earth.

Frequently, it is convenient to think in terms of the diffusion coefficient in B-L space, D_L. The conversion from D_{α} to D_L is straightforward (cf. Birmingham, 1969).

$$D_L = L^4 D_{\alpha}/\mu^2 \tag{9}$$

B. Transformation of the Solution of the Diffusion Equation

Most authors who have worked on the diffusion problem have simply solved equation (8) and correlated the results with data. However, one gets a better feeling for the physical processes by comparing quantities which have a readily apparent physical meaning. The perpendicular flux is a quantity which is more nearly related to the actual output of the detector than $\langle Q \rangle$. For this reason, it was decided to solve (8) at a given J for a family of M. The resulting values of $\langle Q \rangle$ can then be transformed and integrated to give the perpendicular flux in a manner analogous to the inverse procedure given in the next section. The result is a predicted flux along a locus of constant J for all α. The procedure is then repeated for a different J, and in this way the diffusion pattern for all space is built up from one-dimensional cuts. The final result is presented in ordinary B-L or R-λ space as contours of predicted perpendicular fluxes. Direct comparisons can then be made with the actual flux.

C. Conversion of J to $\langle Q \rangle$

Now we must trace the tortuous path from counting rates to the rather obscure $\langle Q \rangle$. First, the perpendicular flux is calculated in the manner already described. Then, this perpendicular flux must in turn be converted to flux differential in energy. This step makes use of the spectral parameter, N. Lavine and Vette calculate N-1 where

$$J(>E,B,L) = J(>E_1,B,L)(E/E_1)^{-(N-1)} \qquad (10)$$

Let this be simplified by defining $\Phi(B,L)$ such that

$$J(>E,B,L) = \Phi(B,L)E^{-(N-1)} \tag{11}$$

The counting rate, C, is given by

$$C(B,L) = [\, J(>40) - J(>110)\,]\epsilon\, G(N) \tag{12}$$

The product, $\epsilon\, G(N)$ is given in Figure 5. Substituting equation (11) into (12) gives the result

$$C(B,L) = \epsilon\, G\Phi[\, 40^{-(N-1)} - 110^{-(N-1)}\,] \tag{13}$$

Equation (13) can now be solved for Φ and the result substituted back into equation (10).

$$J(>E,B,L) = \epsilon\, GCE^{-N}/[\, 40^{-(N-1)} - 110^{-(N-1)}\,] \tag{14}$$

Now the differential flux, j, can be calculated directly from (14).

$$j = -\frac{dJ}{dE} = C(N-1)\epsilon\, GE^{-N}/\,[\, 40^{-(N-1)} - 110^{-(N-1)}\,] \tag{15}$$

To continue further, we need a relation between j and $\langle Q \rangle$. Nakada and Mead found such a relation valid on the equator (although for a slightly different space), but Birmingham gives a relation which is valid off the equator also. Rather satisfyingly, the two relations can be shown to be equivalent. Birmingham's expression is

$$\langle Q \rangle = (\pi/2)(j/E) \tag{16}$$

However, to use equation (16) to convert from j to $\langle Q \rangle$ one must be careful to evaluate j (which in this expression, is not necessarily

perpendicular to B) along to proper solid angle specified by M, J, and α. In this study, the initial conditions are specified to make the proper solid angle perpendicular to the line of force.

D. Coordinates

Although the diffusion described here is one dimensional, it takes place in the two dimensional B-L space. Therefore, the paths of particles drifting inward must be specified by two parameters, and B and L are not particularly convenient for this purpose. One coordinate is determined by equation (8). That is α.

The second coordinate is a special one designed to have a readily apparent physical meaning, and to be convenient to use in a computer program. Consider that the locus of mirror points traced out by a particle as it drifts inward is approximately a line of constant magnetic latitude. This locus is called a line of constant K where K is an adiabatic invariant derived from the first two invariants (McIlwain, 1966a). Traces of constant K are shown in Figure 9. K, however, is not a convenient parameter to use. Instead, the magnetic latitude at which a given line of constant K crosses a given radial distance from the earth ($= R_{min}$) will be used. Then equation (8) can be solved for discrete values of magnetic latitude, λ, over the full range of α to map out a complete B-L diffusion pattern.

E. Boundary Conditions

Before solving the equation, certain boundary conditions must be established. Since almost any distribution can be fitted if one varies enough parameters, certain simplifying assumptions have been

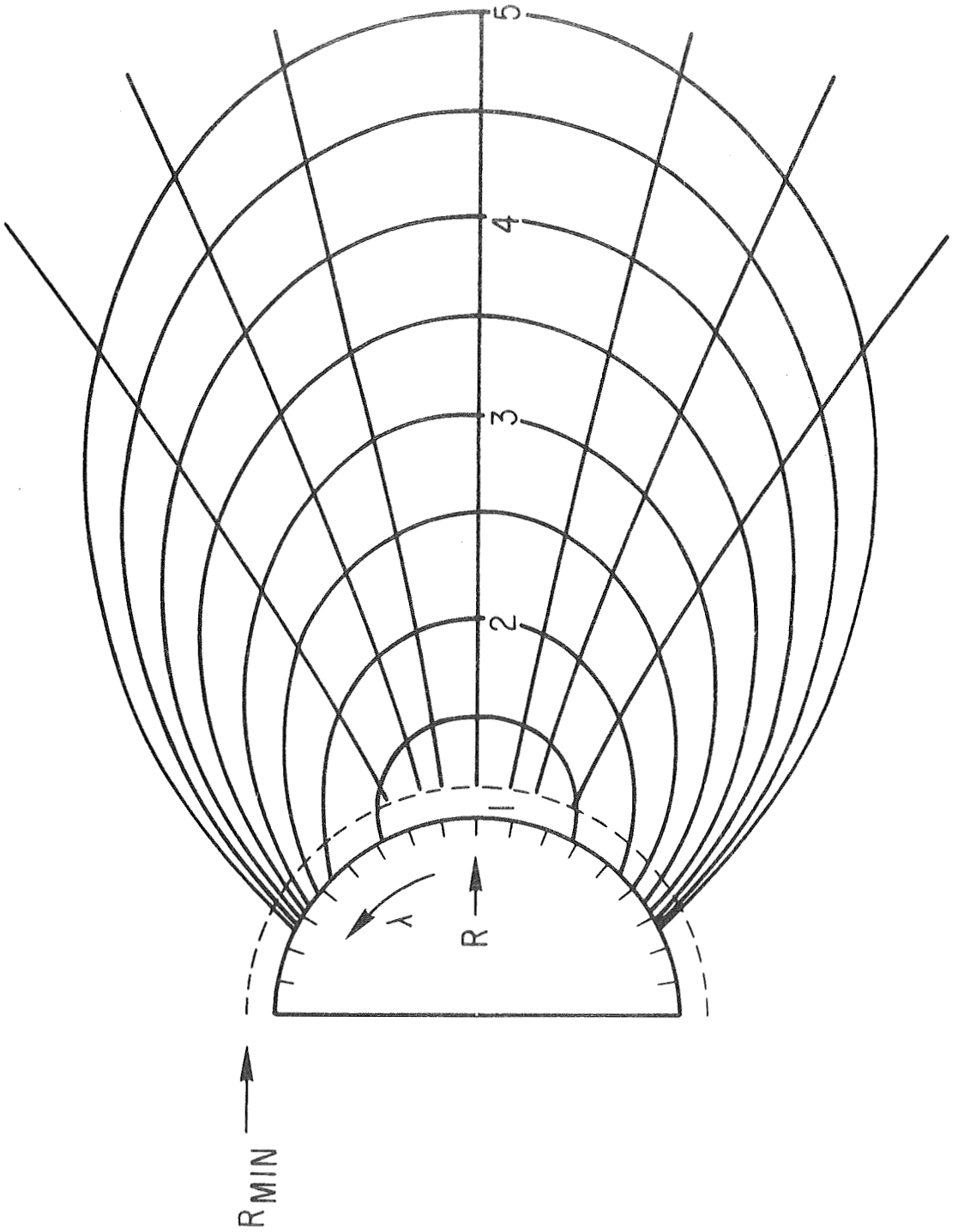


Figure 9 Traces of Constant K in R-λ Space

made about the appropriate boundaries, and these assumptions have been maintained throughout the study.

(1) $\langle Q \rangle = 0$ at R = 1.15 earth radii
(uniform, thick atmosphere with sharp edge).

(2) $\langle Q \rangle$ = constant at $L = L_{max}$
(constant input of new particles on an outer line of force).

(3) $\langle Q \rangle$ specified at the initial time by Injun III and Explorer 15.

(4) S = 0 (no distributed sources or sinks)

(5) $D_L = \Gamma(\lambda) L^{a+4} M^b$

(6) $\langle Q \rangle$ is specified at the final time by Explorer 26.

Condition (6) is not really a boundary condition of the problem, but the criteria against which the solution is weighed. Conditions 1 through 4 are self-explanatory, but the important assumption about the form of the diffusion coefficient needs some elaboration. Fälthammar (1968) has derived two forms for D_L valid throughout space. The first is produced by magnetic fluctuations.

$$D_{Mag} = \Gamma_M(\lambda) L^{(6-2n)} M^{(2-n)} \tag{17}$$

The important new parameter, n, gives the shape of the power spectrum of the disturbances. That is, $P \propto \nu^{-n}$ where ν is the frequency of the disturbance. Similarly, the diffusion coefficient for the electric field disturbances is derived from Fälthammar's equation (25).

$$D_{el} = \Gamma(\lambda) L^{(6-n)} M^{(-n)} \tag{18}$$

Fälthammar gives a plot of $M(\lambda)$, and shows that it drops by a factor of 10 between $\lambda = 0$ and 40°. On the other hand, the proportionality factor for equation (18) is approximately constant throughout space. This provides a powerful tool for determining the driving force of the diffusion (if it exists). The approach is to vary n and Γ for diffusion on the equator until a best fit is found for both equations (17) and (18). Then, holding n constant at the optimum value, go off the equator and determine the best value of Γ as a function of λ. This procedure gives the diffusion coefficient for all space and should enable one to test the importance of diffusion by violation of the third adiabatic invariant as well as determine the source.

Note that in the magnetic case, $n = 2$ gives the familiar L^{10} diffusion, but that pure L diffusion can occur in the elective case only if $n = 0$, and this gives L^{6} diffusion. Magnetic disturbances not infrequently take the form of a rapid rise followed by a long decay. If this decay is long compared to the drift time, then the power spectrum does have $n = 2$ (at least in the region of $\nu = 1/\tau_d$, the drift time). Disturbances with a short rise and fall time have $n = 0$. Therefore, we find that the most likely diffusion coefficients do indeed depend only on L and not on M. Of course, this speculation must be investigated by solving the diffusion equation before any physical truth can be assigned to it.

F. Determination of Γ

In practice, the best way to find Γ has been to select n, and then actually solve the diffusion equation for various values of Γ.

The best fit is defined by a procedure described in the next section, and the Γ used for that fit is adopted as the best value. Therefore, we should look in detail into the way Γ is found. The diffusion equation (8) can be rewritten with the assumed form of D_L as

$$\frac{\partial \langle Q \rangle}{\partial t} = \frac{\partial}{\partial \alpha} \left[\mu^2 (\Gamma L^a M^b) \frac{\partial \langle Q \rangle}{\partial \alpha} \right] \tag{19}$$

where a and b are determined by (17) or (18). Then, let

$$\tau = t\Gamma \tag{20}$$

and

$$A = 1/L = -\alpha/\mu \tag{21}$$

Substitution into equation (19) yields

$$\frac{\partial \langle Q \rangle}{\partial \tau} = \frac{\partial}{\partial A} \left[(L^a M^b) \frac{\partial \langle Q \rangle}{\partial A} \right] \tag{22}$$

This equation is now solved by means of a FORTRAN subroutine, PARAB, which is a highly modified version of an ALGOL procedure, PARABI (Gram, 1962). PARAB solves the difference equation associated with (22) to any accuracy specified in advance. PARAB sets the mesh size in both distance and time automatically to give the desired accuracy with the minimum number of calculations.

When a normalized time, τ, is found which satisfies the fit criteria given in the next section, Γ can be found by means of equation (20) and the fact that $t = 1096$ (that is, from January 1, 1963 to January 1, 1966 is 1096 days).

G. Determination of Quality of Fit

Before continuing on the results, we must give careful attention to the method of deciding on the best fit. Simply "eyeballing" the results may give the same answer as a more sophisticated selection method, but very little is learned quantitatively about the quality of fit. However, the next step is sophistication above "eyeballing" is a rather difficult one to take. If one chooses the average value of the ratio of the predicted counting rates to the measured ones as an error parameter, it will be quickly learned that by predicting no change at all from 1963 to 1966, the error parameter is .925 on the equator (i.e., the average change is small). Now this might not be a bad fit, but it does not tell much about the physics involved. On the other hand, if one adopts for an error parameter the average value of the ratio of the predicted change in counting rates to the measured change in counting rate, he will discover that the denominator is zero or at least very small at several locations. Therefore, this error parameter will always be infinitely large regardless of the quality of fit. Again no physics.

Within about 10° of the equator, the possibility exists for establishing a morphological criteria for a good fit. In Figures (10) and (11) are plotted the directional fluxes for 1963 and 1966 respectively. Note that both exhibit a secondary peak near the equator which moves inward in L as time progresses. One could simply allow the diffusion to continue until the peak in the predicted rates matched the peak in the measured rates. If one is very fortunate, the minima will match up at the same time. The inner, large peak is almost useless in

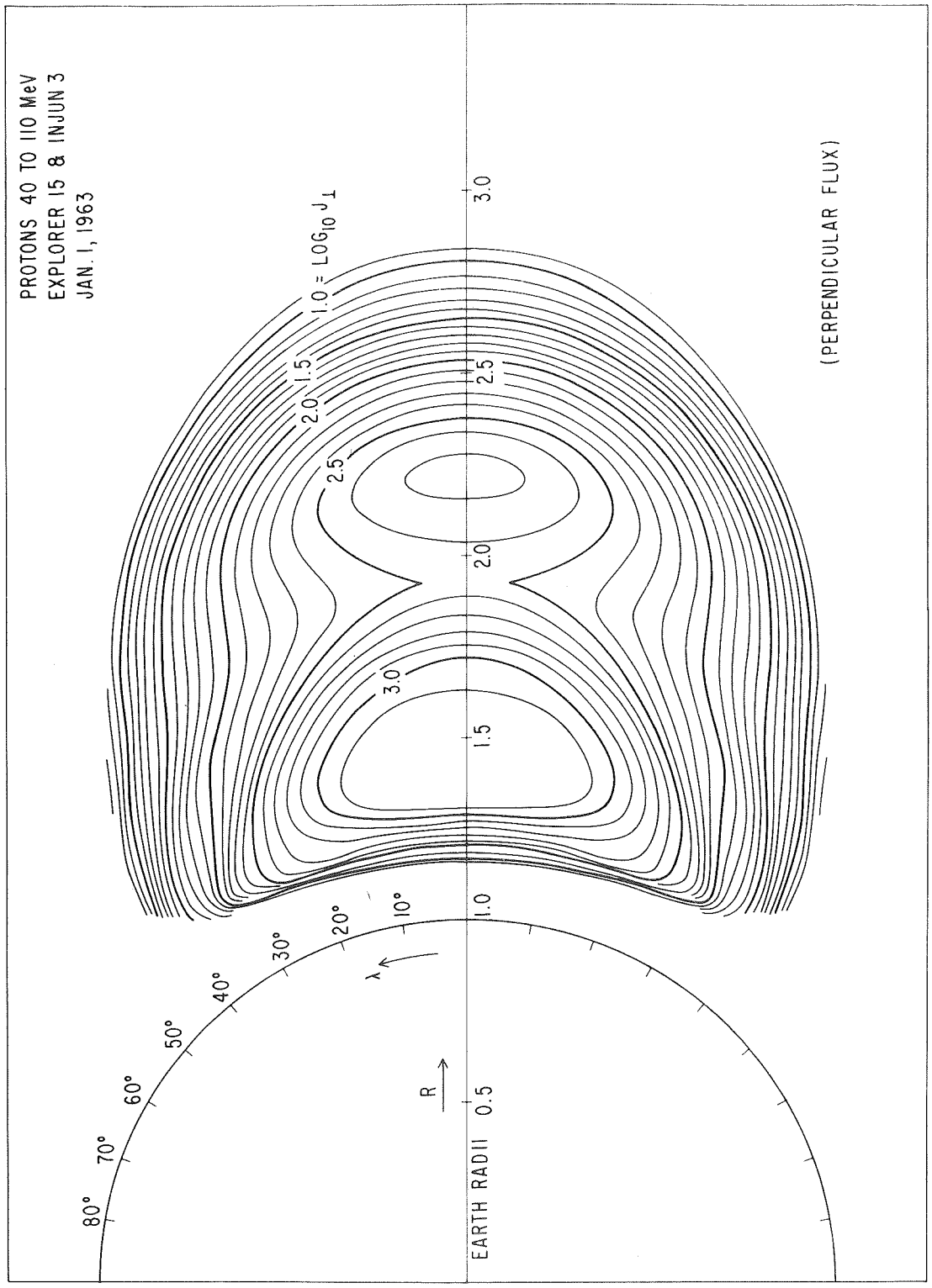


Figure 10 Directional Flux for January 1, 1963 (R-λ)

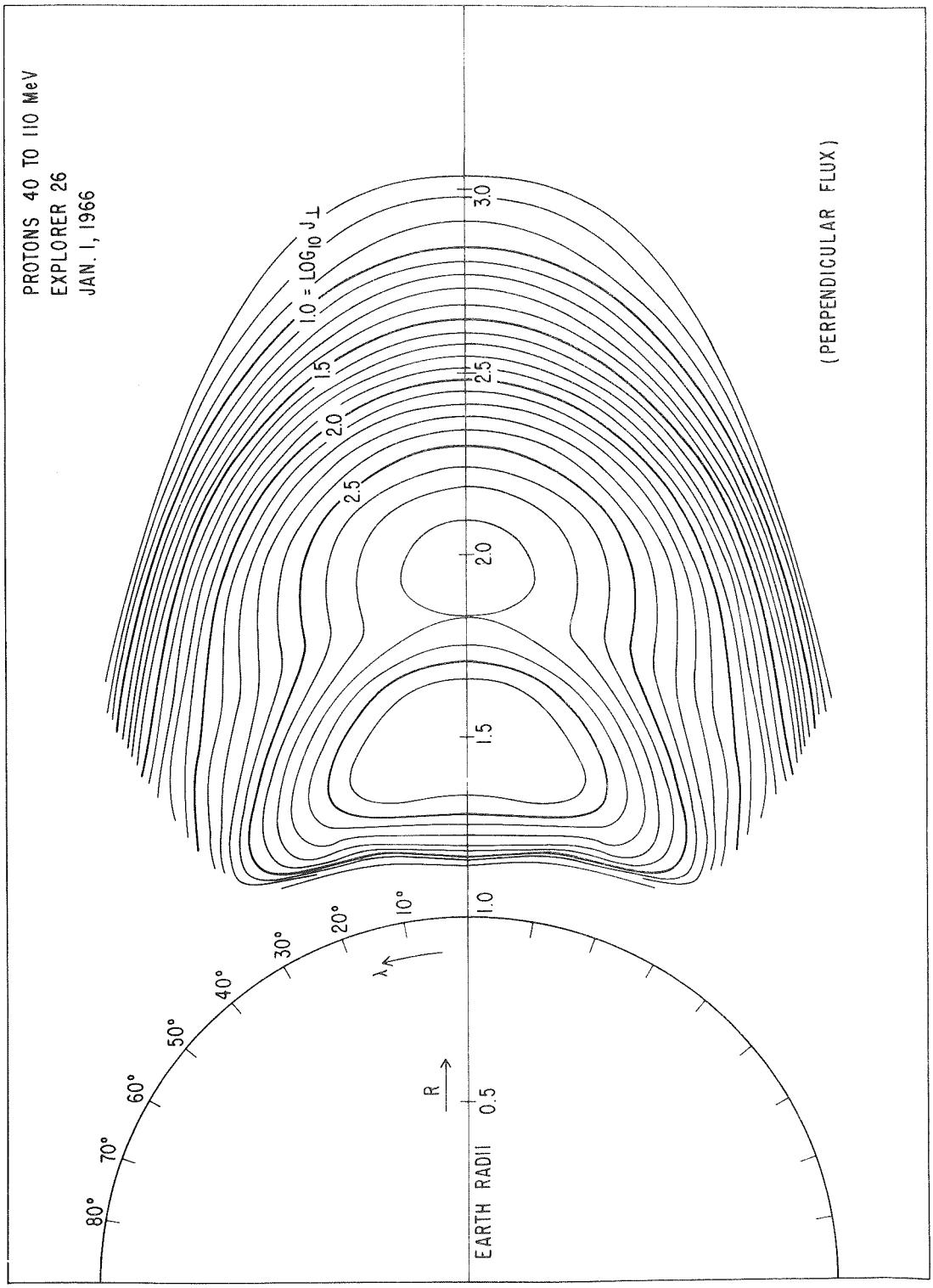


Figure 11 Directional Flux for January 1, 1966 (R-λ)

this sense since it does not move as much. Therefore, we must return to the first suggestion to try to find a reasonable criteria which works over all space.

The first thing to note is that even though the average value of the ratio of the predicted to measured counting rates gives .925 for no change at all, the counting rates actually do change by more than a factor of 3 in some places. Therefore, the %RMS deviation about .925 must be very large. However, if the diffusion theory is giving correct results, then this average ratio should be close to 1 and the %RMS deviation should be small. So the average ratio is a good error parameter provided we look for a minimum in the %RMS deviation at the same time.

Data points used to form the average ratios are only taken from $L < 2.15$ to R_{min} near the equator and $L < 1.95$ near $\lambda = 30$. This avoids the region of nonadiabatic losses mentioned in the Introduction.

The situation is a bit less straightforward in calculating a reasonable average ratio of the change in predicted counting rates to the measured rates. The best compromise has been to disregard any data points which change by less than 8% of the 1963 counting rate. This figure of 8% was chosen empirically by noting that the ratio became very large for those data points which did not satisfy this condition, even when the fit "looked" good. However, to be on the safe side, it is best to consider the %RMS deviation about the average value in this case also. One would expect a minimum in the %RMS deviation at the position of best fit.

Of 108 possible points that could be used to form this average, 40 are eliminated by the 8% test on the equator. As λ increases, less points are eliminated.

As we shall see in the next section, all of these errors are equivalent. That is, the position of the peaks match at the same time that the minima match, the %RMS deviation in the average ratio of rates is a minimum, and the %RMS deviation in the average ratio of the change in rates is a minimum, all at the same time. Further, this happens when the fits "look" good, and when both the average ratios are nearly equal to 1. This is very convenient since the two ratios do not necessarily actually equal 1 at the same time. Therefore, this combination approach avoids soul-searching decisions as to which ratio is the better indicator, or if one is better than the other at certain locations.

V. RESULTS AND CONCLUSIONS

A. Equator

The search for the best value of the spectral parameter, N, on the equator gave unambiguous results for both the electric and magnetic cases. $L^6(N = 0)$ gives the best fit for the electric case, and L^{10} $(N = 2)$ gives the best fit for the magnetic case. The results are shown in Figure 12 for the two cases mentioned and for N = 1 in the electric case.

The differentiation in the quality of fit for various spectral parameters is indicated by the fact that the average ratio of predicted to measured flux is 1.09 ± .16 for L^{10}, and about 1.06 ± .10 for both L^6 and L^5M^{-1}, but drops to .93 ± .24 for L^4M^{-2}. The fits get progressively worse for higher values of N.

In spite of the fact that L^6 and L^5M^{-1} diffusion coefficient give approximately the same average ratio, Figure 12 shows that L^6 matches the functional form of the measured flux somewhat better than L^5M^{-1}.

A question that is frequently asked is how far does a given particle drift. This is answered indirectly by noting the number of time iterations PARAB took to get the result. Then, knowing the step size in α, one can set an upper limit to the propagation distance. The result for a drift time of three years is

$$\Delta(1/L) \leq .05 \tag{23}$$

or

$$\Delta L \leq .05\ L^2 \tag{24}$$

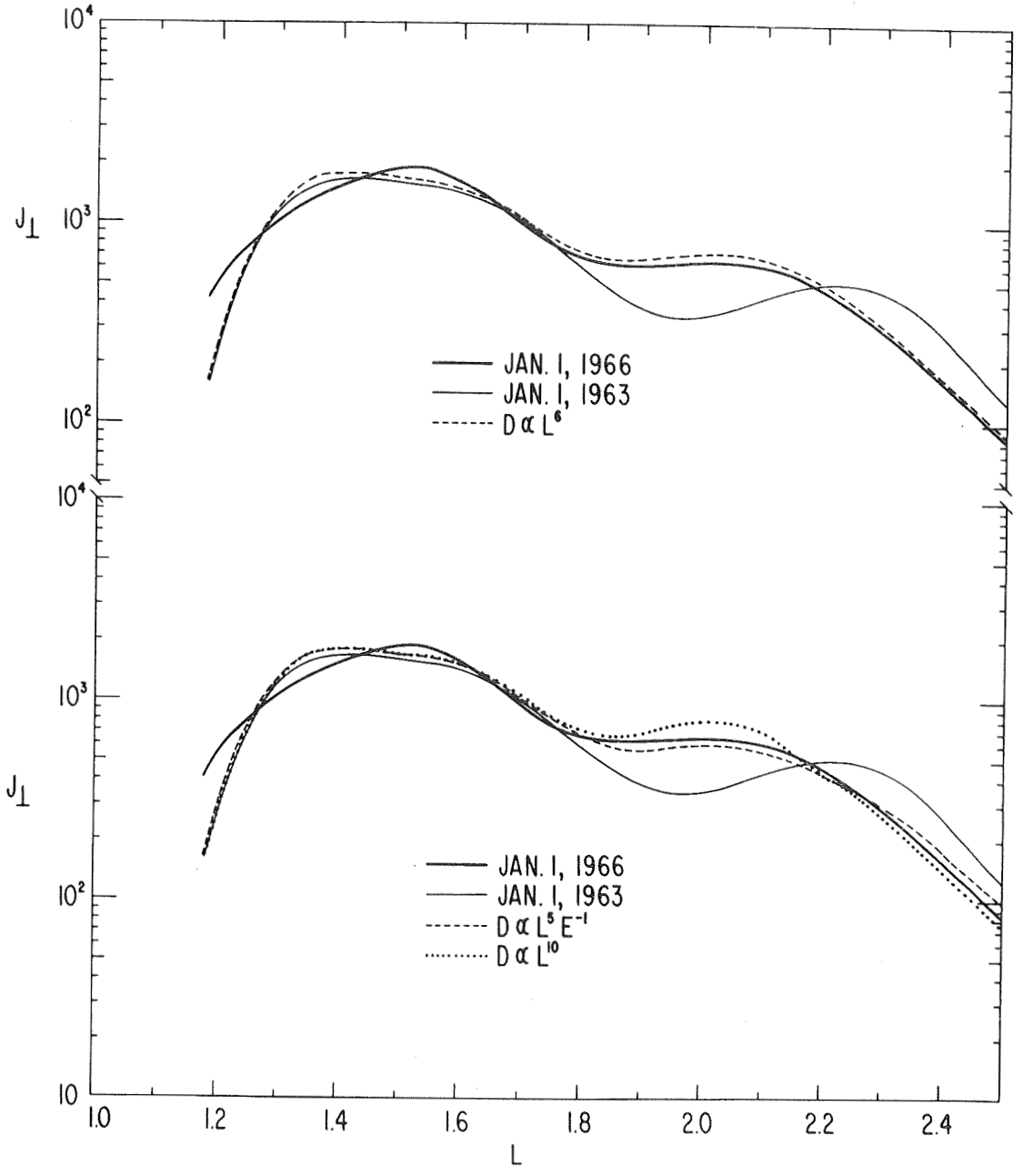


Figure 12 Solutions on the Equator for Differing Forms of the Diffusion Coefficient

This explains why the outer boundary condition is not as critical as the inner one. The usable input data ends at about L = 2.75. Information about the flux at this point will only propagate inward to about L = 2.35 in 3 years. Therefore, any reasonable extrapolation of the flux out to a fixed source will not affect the results greatly.

Equation (2) also helps to explain why all solutions tend to give large deviations from the measured fluxes at the lowest values of L. Since the particles move very little in the range of $L \leq 1.25$, the large changes in counting rate must be due to the effects of the atmosphere, and the atmosphere has not been treated entirely correctly. By forcing the counting rates to be zero at R = 1.15, two kinds of approximations are made. First, no allowance is made for the decrease in residual atmospheric density in 1966 (which is a period of low solar activity) relative to 1963 (which is just after the solar maximum). Blanchard and Hess (1964) calculated the effect of variation of the atmosphere on trapped particles and found that the density at L = 1.25 (about 3×10^3 oxygen atoms equivalent/cm^3 at solar minimum) varies by about a factor of 100 on the equator. Also the atmosphere should be treated as a distributed loss term to account properly for its effect on particles. However, the addition of this refined loss term to the diffusion equation complicates the solution sufficiently that its utility is highly questionable.

For the purposes of the present work, it can be noted that the low predicted counting rates in the range $L < 1.25$ are probably due to the decreased loss to the atmosphere, and the excess counts predicted

in the range $1.25 \leq L \leq 1.43$ are probably due to neglecting losses produced by the residual atmosphere.

Also from Figure 12, we can estimate the total losses not accounted for in the range of $L \leq 1.65$ as approximately 3% per year, since the predicted curve falls above the measured one by that much.

This leaves unexamined only the range of $1.43 < L < 1.65$, where the predicted rates are too low. The most likely reason for this discrepancy is that a source of particles has not been accounted for in the solution. Perhaps the source could be from neutron decay. If so, we can say that CRAND has a net effect of adding only about 3% per year over a very limited spatial extent.

The best values of D_L that goes with the best fit in Figure 12 is

$$D_L = 1.32 \times 10^{-7} L^6 \left[R_e^2/\text{day} \right] \tag{25}$$

By comparison, Williams (1970) gives

$$D_W = 2.4 \times 10^{-9} L^{10} \left[R_e^2/\text{day} \right. \tag{26}$$

The diffusion coefficient for the electric case is equal to Williams value at

$$L = \left(\frac{1.32 \times 10^{-7}}{2.4 \times 10^{-9}} \right) = 2.72 \tag{27}$$

Since the development so far seems to give results in reasonable agreement with other workers, we now proceed to find $\Gamma(\lambda)$ for the L^6 case.

B. $\Gamma(\lambda)$ and Electric Field Strength

To demonstrate the overall quality of fit both on and off the equator, Figure 13 shows the ratio of measured 1966 fluxes and predicted 1966 fluxes to measured 1963 fluxes.

The variation of Γ with λ is shown in Figure 14, but to facilitate comparison with predictions of magnetic fluctuations, the ratio of $\Gamma(\lambda)/\Gamma(0)$ is plotted instead of $\Gamma(\lambda)$. The indicated error bar gives the spread due to the different methods of determining the best fit, and due to the discrete values of diffusion times that were used. On the equator, all of the different methods agreed to within the accuracy of the calculations, so no error bar is shown. The lower limit in the first four points (all at $\lambda < 10$) was set by matching the positions of the outer peak. The absolute error in $\Gamma(\lambda)$ for their first points probably agrees well with the indicated error bars. However, for the higer values of λ, the exact method of handling the data becomes more critical and the net error increases. Therefore, the outer points at $\lambda > 25^{\circ}$ are probably only accurate to within 50%. In this context, it is interesting to note that including regions of space with known non-adiabatic losses in the calculation decreases $\Gamma(25^{\circ})$ by a factor of 4. However, the value of $\Gamma(0)$ is affected only slightly by the inclusion of these regions.

Even with these allowances, it is obvious that the measured shape of the $\Gamma(\lambda)$ curve cannot be explained by magnetic variations alone. (A similar result is obtained if L^{10} diffusion is used.)However, in trying to explain the shape of $\Gamma(\lambda)$, one finds that the assumption of the spectral power density varying like ν^{-n} is not a good one. A

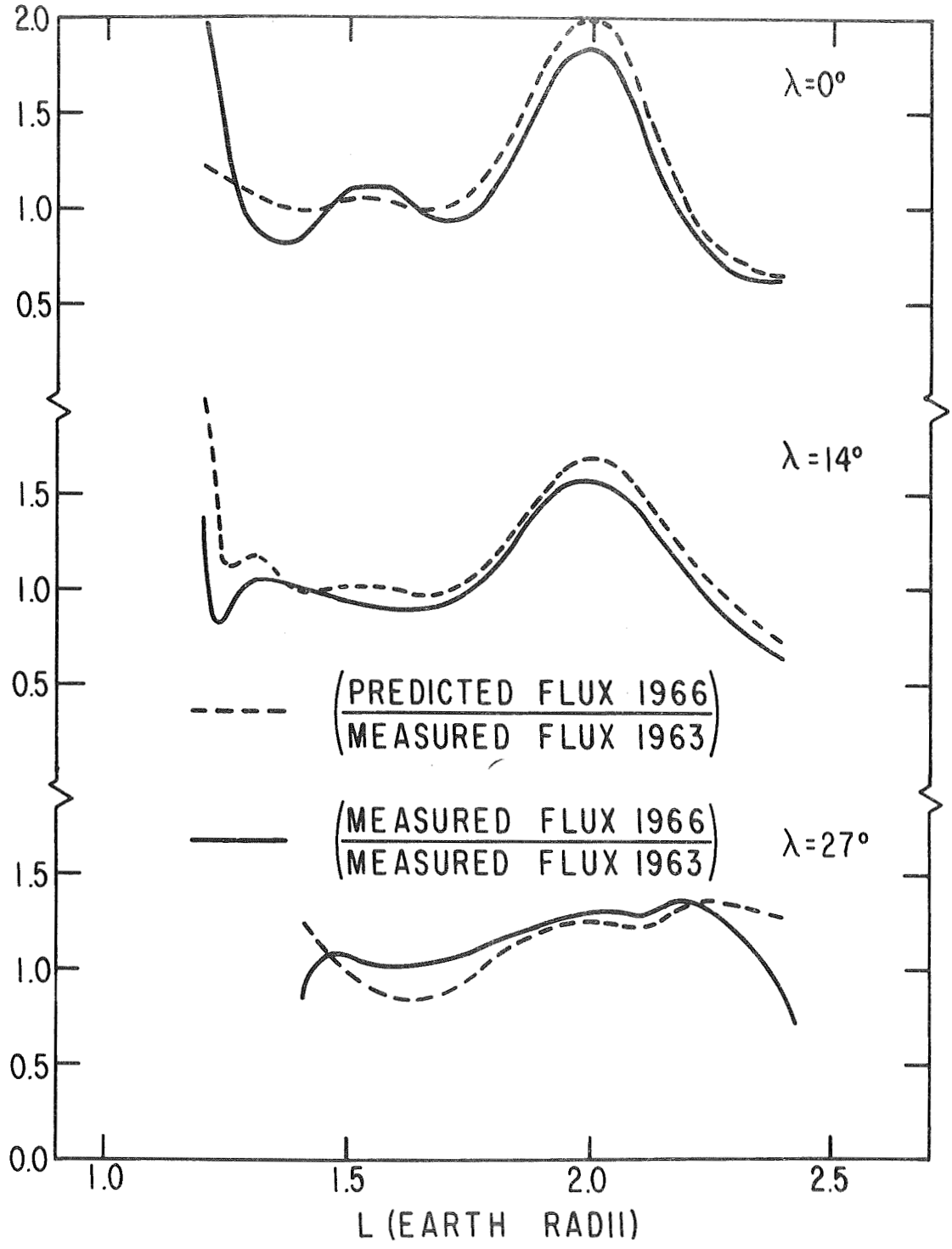


Figure 13 Ratio of Predicted to Measured Fluxes on January 1, 1966

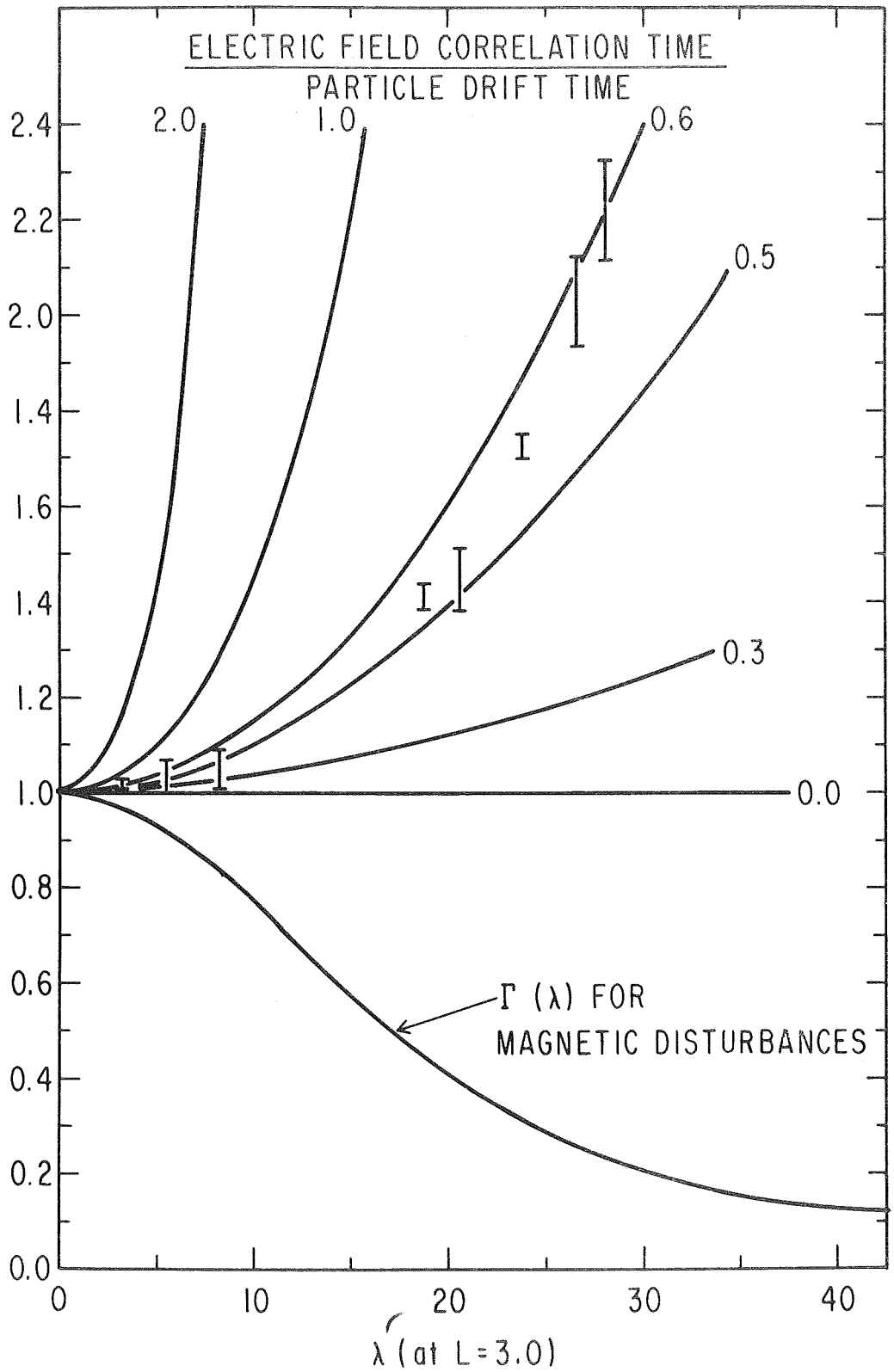


Figure 14 Latitudinal Dependence of the Diffusion Coefficient

better fit is obtained if we consider an assumption made by Birmingham (1964) which can be written,

$$D_L = [\, A\pi^{\frac{1}{2}} c^2 L^6 T_c / 4\mu^2 \,]\, e^{-\pi^2 (T_c/T_d)^2} \qquad (28)$$

where A is the square of the fluctuating electric field strength, T_c is the correlation time of the fluctuation, and T_d is the drift period of the particles. The assumptions here, as Birmingham states, are similar to the ones made by Cornwall (1968). That is, the electric field is directed from dawn to dusk and exhibits no periodic variations.

In this model, the electric field magnitude is the same throughout the magnetosphere at any given instant, and T_c is a constant everywhere. Therefore, this new form of the diffusion coefficient adds additional L-dependence since $T_d \propto 1/L$. This means that the diffusion equation should be solved again, and a two-dimensional search made for the best D_L by varying both A and T_c. However, we can avoid that lengthy process if ratio T_L/T_d is small enough throughout the region of interest. Curves based on equation (28) are plotted in Figure 14 for several values of T_c/T_d. The $\Gamma(\lambda)$ curve is seen to be consistent with equation (28) for some small value of T_c/T_d. For the purposes of the following calculation, we will assume $T_c/T_d = .55$, but keeping in mind that this value should be interpreted as an average value. Given their last assumption, A and T_c can be found from the properties of D_L.

Starting from equation (28), let $R = T_\lambda/T_o$,

where T_λ is the drift time at a given λ and T_o is the drift time on the equator, then

$$\frac{\Gamma(\lambda)}{\Gamma(0)} = e^{\pi^2 (T_c/T_o)^2 (1-1/R^2)} \tag{29}$$

An expression for R can be found from the drift time equation derived by Hamlin, et al. (1960),

$$T_\lambda = \frac{2.7 \times 10^9}{.7 + .3 \sin\beta_o} \left(\frac{1}{LE(ev)}\right) \tag{30}$$

where β_o is the equatorial pitch angle, and

$$\sin\beta_o = \left[\cos^6\lambda / (4-3\cos^2\lambda)^{\frac{1}{2}} \right]^{\frac{1}{2}} \tag{31}$$

Equation (29) can be combined with equation (25) to yield

$$D(L,\beta_o) = 1.32 \times 10^{-7} L^6 e^{(.55\pi)^2} \left[1 - (.7+.3 \sin\beta_o)^2 \right] \tag{32}$$

which can be further simplified

$$D(L,\beta_o) = 1.32 \times 10^{-7} L^6 e^{.27(5.67+\sin\beta_o)(1.0-\sin\beta_o)} \tag{33}$$

The evaluation of the electric field is most easily accomplished by noting that Birmingham has calculated that the quantity in brackets in (28) is 1.3×10^{-4} for T_c = 1 hr. and A = $(.2\ mv/m)^2$. This allows us to write

$$1.32 \times 10^{-7} = \left(\frac{1.3 \times 10^{-4} T_c A}{(3600.)(.04)}\right)_e - (.55\pi)^2 \tag{34}$$

where T_c is now in seconds and A in $(mv/m)^2$. A reasonable value of T_c can be calculated from (30) at L = 2.7 for 45 Mev.

$$T_c = \frac{(.55)(2.7 \times 10^9)}{(2.7)(4.5 \times 10^7)} \approx 12.\ sec. \tag{35}$$

When T_c is substituted into (34), the magnitude of the fluctuating field is found to be approximately 0.5 mv/m.

However, care must be taken in trying to put physical significance on the values just calculated. Although the ratio, $T_c/T_d = .55$ fits the data well, it does appear squared in an exponential. Therefore, small errors in the determination of the ratio will result in large errors in both the field strength and correlation time. Also, the additional L-dependence of the diffusion coefficient due to exponential has been neglected. Therefore, in equation (35) we had to assume a characteristic L of 2.7. Because of these effects, the determination of T_c is probably correct only to within an order of magnitude, and the field strength to within a factor of 2.

VII SUMMARY

Direct application of diffusion theory to the fluxes of 40 to 110 Mev geomagnetically trapped protons shows that the data is consistent with a model of diffusion by violation of the third adiabatic invariant. Although no distributed sources or sinks of particles were assumed, much of the residual differences between predicted and measured fluxes can be explained if about 3% per year of the particles are lost at $L > 1.63$ by some undefined mechanism. An upper limit to the net effect of a possible distributed source of particles has been placed at 3% per year at $1.25 < L < 1.43$, and much lower than that elsewhere.

If it is assumed that the diffusion is driven by an electric field of randomly varying magnitude directed from dawn to dusk, then the data has been shown to be consistent with an auto-correlation time of 12 seconds and an average magnitude of .5 mv/m.

APPENDIX

In any study which involves as many transformations as this one has, there are many ways to present the results, and one must use discretion to avoid cluttering the paper proper. For the type of data discussed here, one might logically present the results in R-λ or B-L space, and one might present either the omnidirectional or directional contours. This means there are a total of eight graphs that could be shown of the data. Of these, four have already been presented in the main text. The other four are presented here to complete the set. No new information is contained in these graphs, but the different form of presentation may facilitate understanding the physical processes involved.

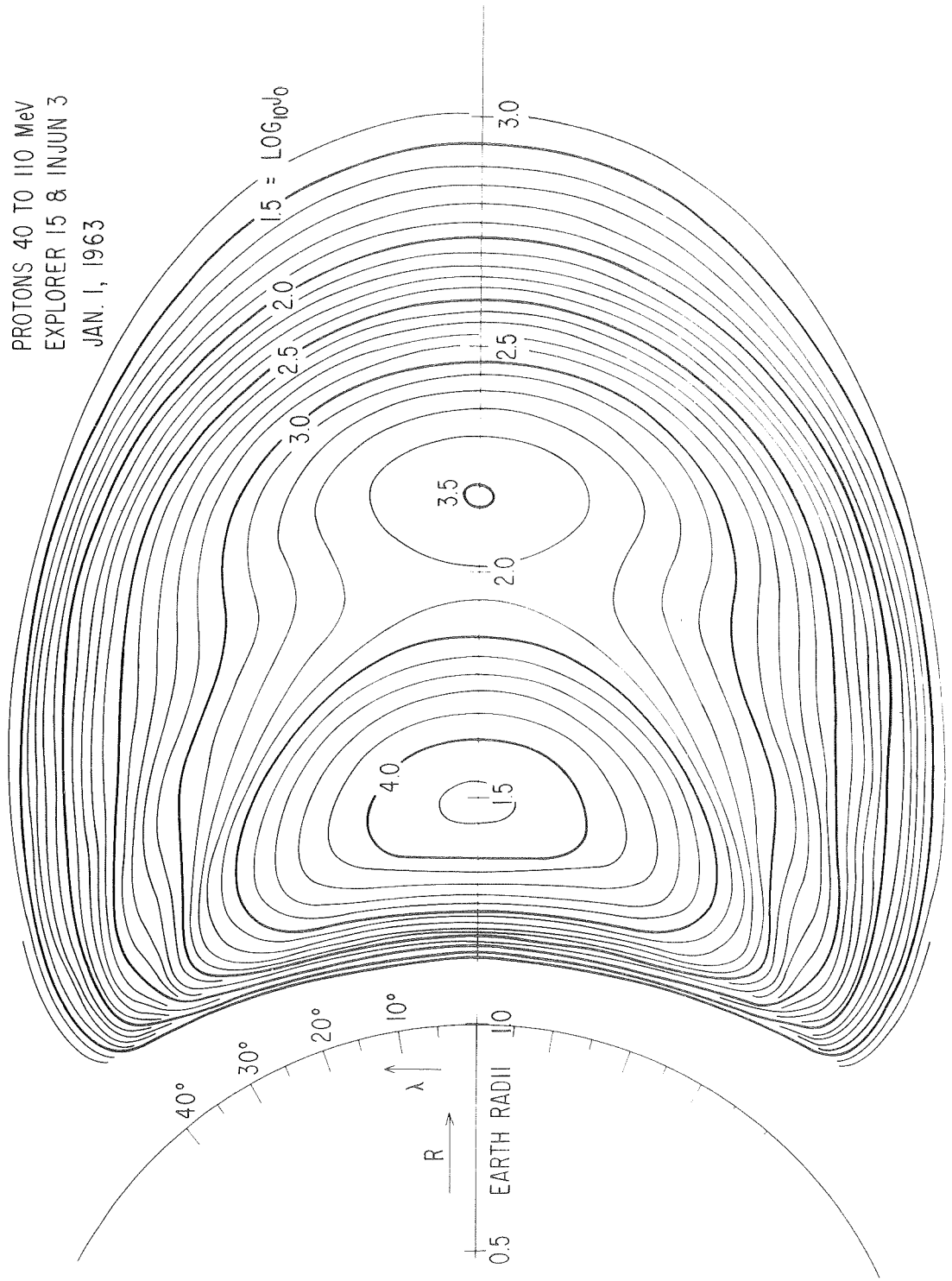


Figure 15 Omnidirectional Flux for January 1, 1963 (R-λ)

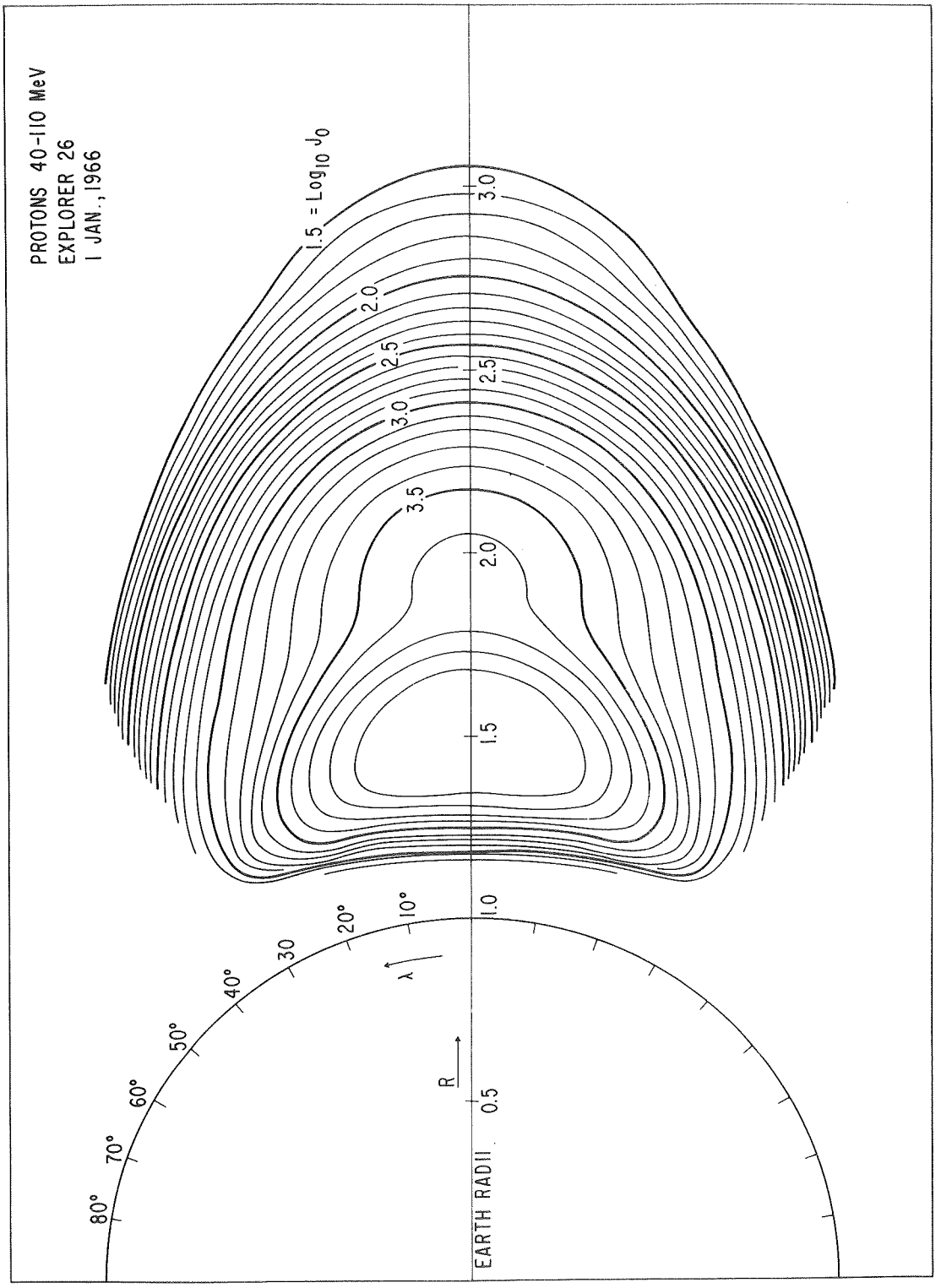


Figure 16 Omnidirectional Flux for January 1, 1966 (R-λ)

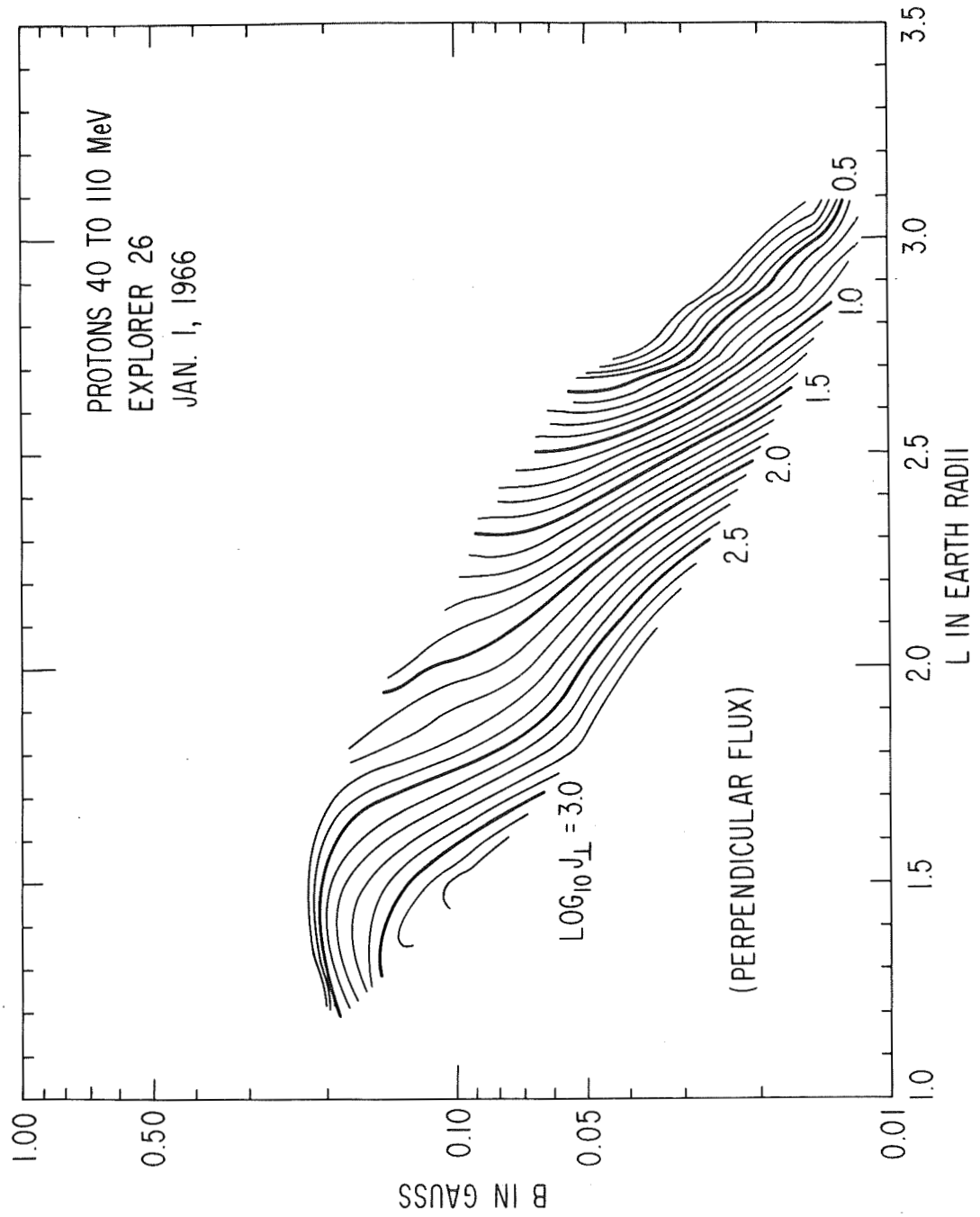


Figure 17 Directional Flux for January 1, 1966 (B-L)

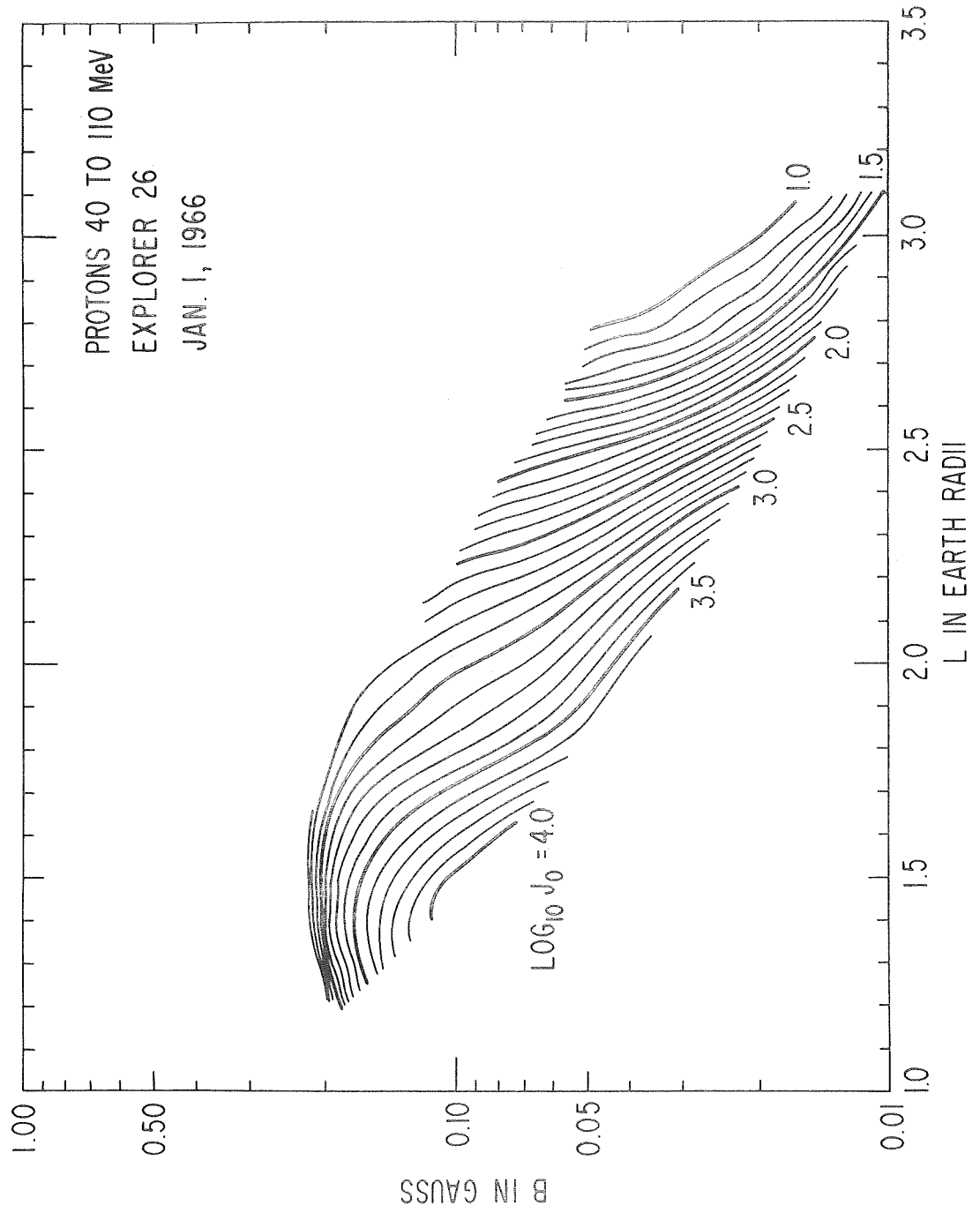


Figure 18 Omnidirectional Flux for January 1, 1966 (B-L)

REFERENCES

Akasofu, S. I., The neutral hydrogen flux in the solar plasma flow, Planetary Space Sci., 12, 905, 1964.

Birmingham, T. J., Convection electric fields and the diffusion of trapped magnetospheric radiation, J. Geophys. Res., 74, 2169, 1969.

Blanchard, R. C., and W. N. Hen, Solar cycle charges in inner-zone protons, J. Geophys. Res., 69, 3927, 1964.

Cornwall, J. M., Diffusion processes influenced by conjugate-point wave phenomena, Radio Sci. 3, 740, 1968.

Davis, L., and D. B. Chang, On the effect of geomagnetic fluctuations on trapped particles, J. Geophys. Res., 67, 2169, 1962.

Davis, L. R., and J. M. Williamson, Low-energy trapped protons, Space Research, 3, 365, North-Holland Publishing Co., 1963.

DeForest, S. E., Effects of different field expansion on omnidirectional proton counting rate data, J. Geophys. Res. 71, 3273, 1966.

DeForest, S. E., Precipices and chasms in the magnetospheric plasma, E.O.S., 51, 390, 1970.

Dragt, A. J., M. M. Austin, and R. S. White, Cosmic ray and solar proton albedo neutron decay injection, J. Geophys. Res., 71, 1293, 1966.

Fälthammar, C-G., On the transport of trapped particles in the outer magnetosphere, J. Geophys. Res., 71, 1487, 1966.

Fälthammar, C-G., Radial diffusion by violation of the third adiabatic invariant, Earth's Particles and Fields, 157, Reinhold Book Corp., New York, 1968.

Fälthammar, C-G., Introductory survey of radiation-belt diffusion, presented at the Advanced Study Institute, Earth's Particles and Fields, Santa Barbara, Cal., 1969.

Farley, T. A., and N. L. Sanders, Pitch angle distributions and mirror point densities in the outer radiation zone, J. Geophys. Res. 67, 2159, 1962.

Fillius, R. W., Penetration of solar protons to four earth radii in the equatorial plane, Annales de Géophysique, T. 24, fasc. 3, 821, 1968.

Freden, S. C., and R. S. White, Protons in the earth's magnetic field, Phys. Rev. Letters, 3, 9, 1959.

Freden, S. C., and R. S. White, Particle fluxes in the inner radiation belt, J. Geophys. Res., 65, 1377, 1960.

Gram, C., Selected Numerical Methods, Regnecentraten, Copenhagen, 1962.

Hamlin, D. A., R. Karplus, R. C. Vik, and K. M. Watra, Mirror and azimuthal drift frequencies for geomagnetically trapped particles, J. Geophys. Res. 66, 1, 1961.

Hess, W. N., and J. Killeen, Spatial distribution of protons from neutron decay trapped by the geomagnetic field, J. Geophys.Res. 71, 2799, 1966.

Hess, W. N., The radiation belt and the magnetosphere, Blaisdell Publishing Co., Waltham, Mass., 1968.

Jenkins, R. W., Simultaneous measurement of the neutron leakage flux in the 0.01-1 and 1-10 Mev energy range, EOS, 51, 394, 1970.

Kellogg, P. J., Van Allen radiation of solar origin, Nature, 183, 1295, 1959.

Levine, J. P., and J. I. Vette, Models of the trapped radiation environment, Volume V: Inner belt protons, NASA Publication, NASA SP-3024, 1969.

McIlwain, C. E., Redistribution of trapped protons during a magnetic storm, Space Research V, 374, John Wiley & Sons, New York, 1964.

McIlwain, C. E., Magnetic Coordinates, Space Sci. Rev. 5, 585, 1966a.

McIlwain, C. E., Measurement of trapped electron intensities made by the Explorer 15 Satellite, Radiation Trapped in the Earth's Magnetic Field, D. Reidel Publishing Co., Dordrecht-Holland, 1966b.

McIlwain, C. E., Equitorial Observation of auroral plasma, EOS, 51, 389, 1970.

Nakada, M. P., J. W. Dungey, and W. N. Hess, Theoretical studies of protons in the outer radiation belts, J. Geophys. Res. 70, 3529, 1965.

Nakada, M. P., and G. D. Mead, Diffusion of protons in the outer radiation belt, J. Geophys. Res. 70, 4777, 1965.

Northrup, T. and E. Teller, Stability of the adiabatic motion of charged particles in the earth's field, Phys. Rev., 117, 215, 1960.

Parker, E. N., Geomagnetic fluctuations and the form of the outer zone of the Van Allen radiation belt, J. Geophys. Res., 65, 3117, 1960.

Pizzela, G., C. E. McIlwain, and J. R. Van Allen, Time variations of intensity in the earth's inner radiation zone Oct. 1959 through Dec. 1960, J. Geophys. Res., 67, 1235, 1962.

Playboy, 10, No. 1, 90, HMH Publishing Co., Chicago, 1963.

Reif, F., Fundamentals of Statistical and Thermal Physics, McGraw-Hill Book Co., New York, 1965.

Roberts, C. S., On the relationship between the unidirectional and omnidirectional flux of trapped particles on a magnetic line of force, J. Geophys. Res., 70, 2517, 1965.

Van Allen, J. A., Spatial distribution and time decay of the intensities of geomagnetically trapped electrons from the high altitude nuclear burst of July 1962, Radiation Trapped in the Earth's Magnetic Field, D. Reidel Publishing Co., Dordrecht-Holland, 1966.

Williams, D. J., Trapped protons ≥ 100 kev and possible sources, Goddard Space Flight Center, Greenbelt, Maryland, X-646-70-9, 1970.

Yeager, D. M., and L. A. Frank, Large temporal variations of energetic electron intensities at midaltitudes in the outer radiation zone, J. Geophys. Res., 74, 5697, 1964.